Electronic Supplementary Information

Three-State Switching in a Double-Pole Change-Over Nanoswitch Controlled by Redox-Dependent Self-Sorting

Sudhakar Gaikwad, Merve Sinem Özer, Susnata Pramanik, Michael Schmittel*

Center of Micro and Nanochemistry and Engineering, Organische Chemie I,

Universität Siegen, Adolf-Reichwein-Str. 2, D-57068 Siegen, Germany

E-mail: schmittel@chemie.uni-siegen.de

Table of Contents

1. NMR spectra

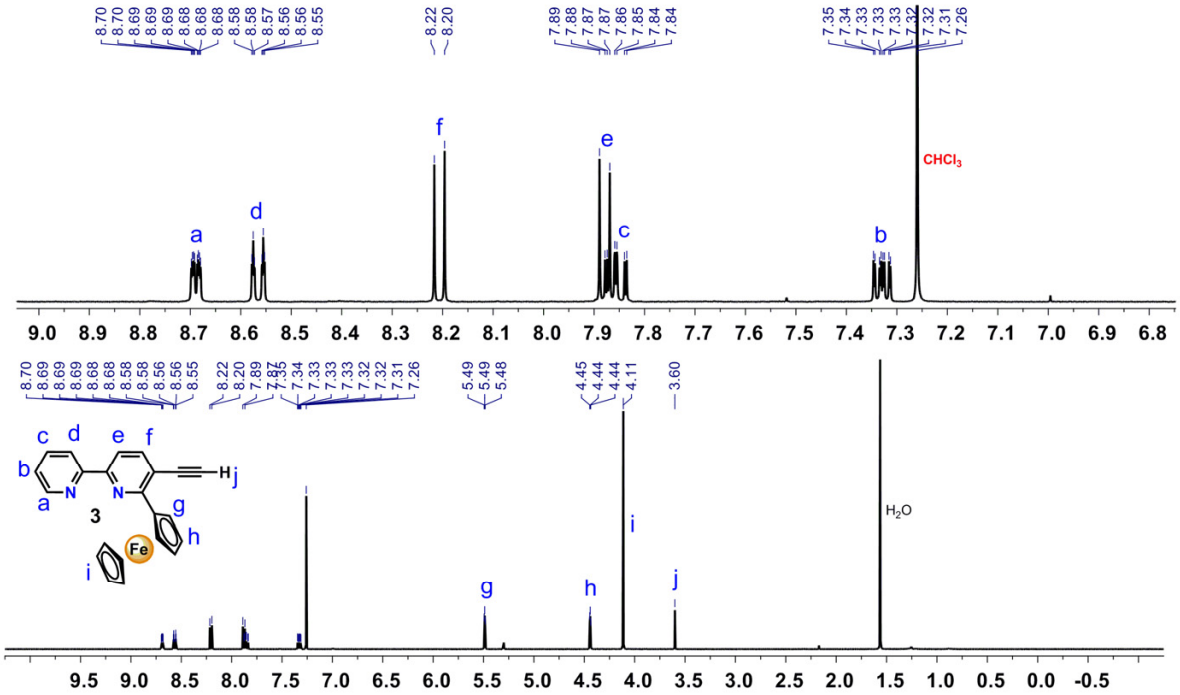

Figure S1. ^{1}H NMR spectrum ($CDCl_3$, 400 MHz, 298 K) of compound **3**.

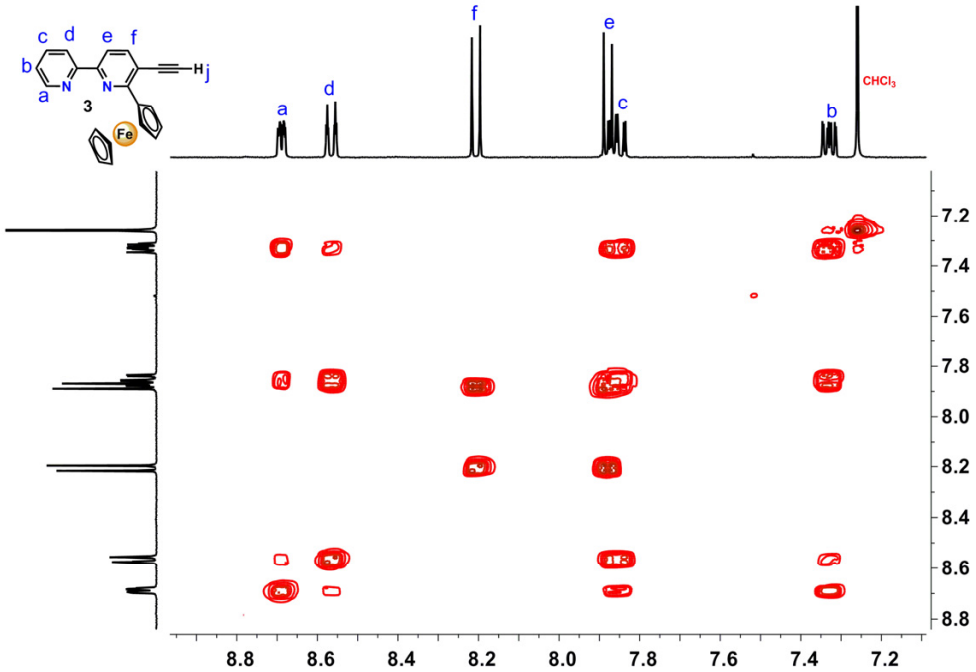

Figure S2. ^{1}H-^{1}H COSY NMR spectrum ($CDCl_3$, 400 MHz, 298 K) of compound **3**.

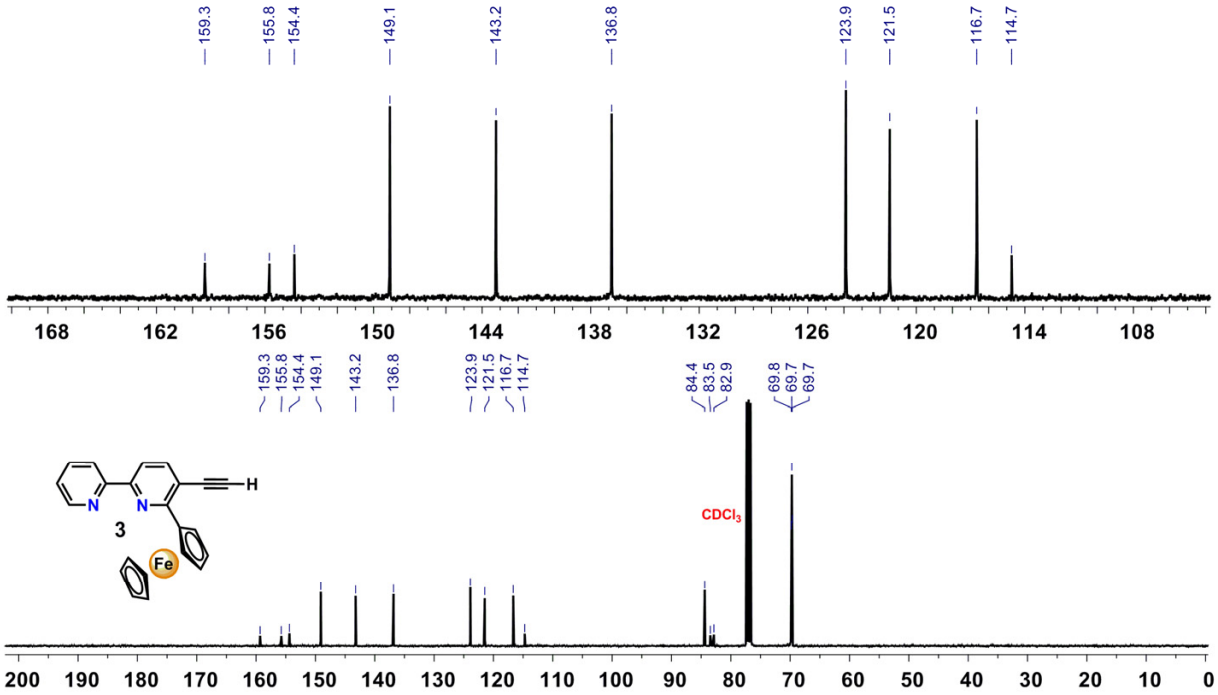

Figure S3. ^{13}C NMR spectrum ($CDCl_3$, 100 MHz, 298 K) of compound **3**.

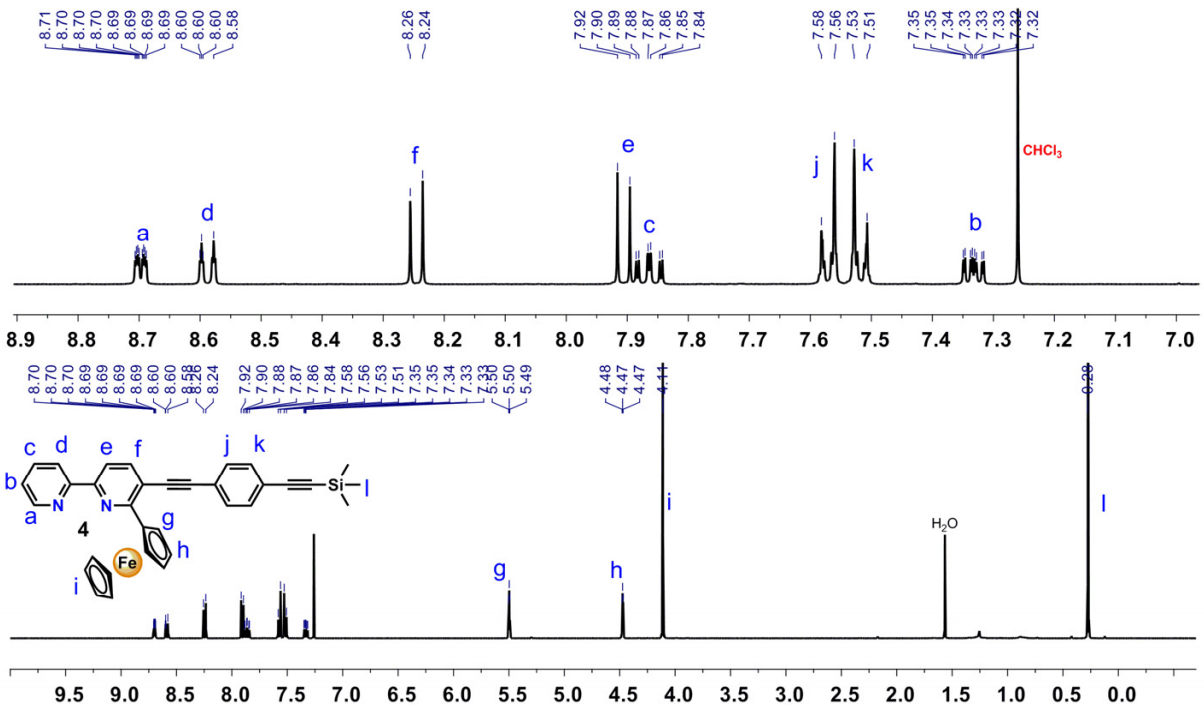

Figure S4. ^{1}H NMR spectrum ($CDCl_3$, 400 MHz, 298 K) of compound **4**.

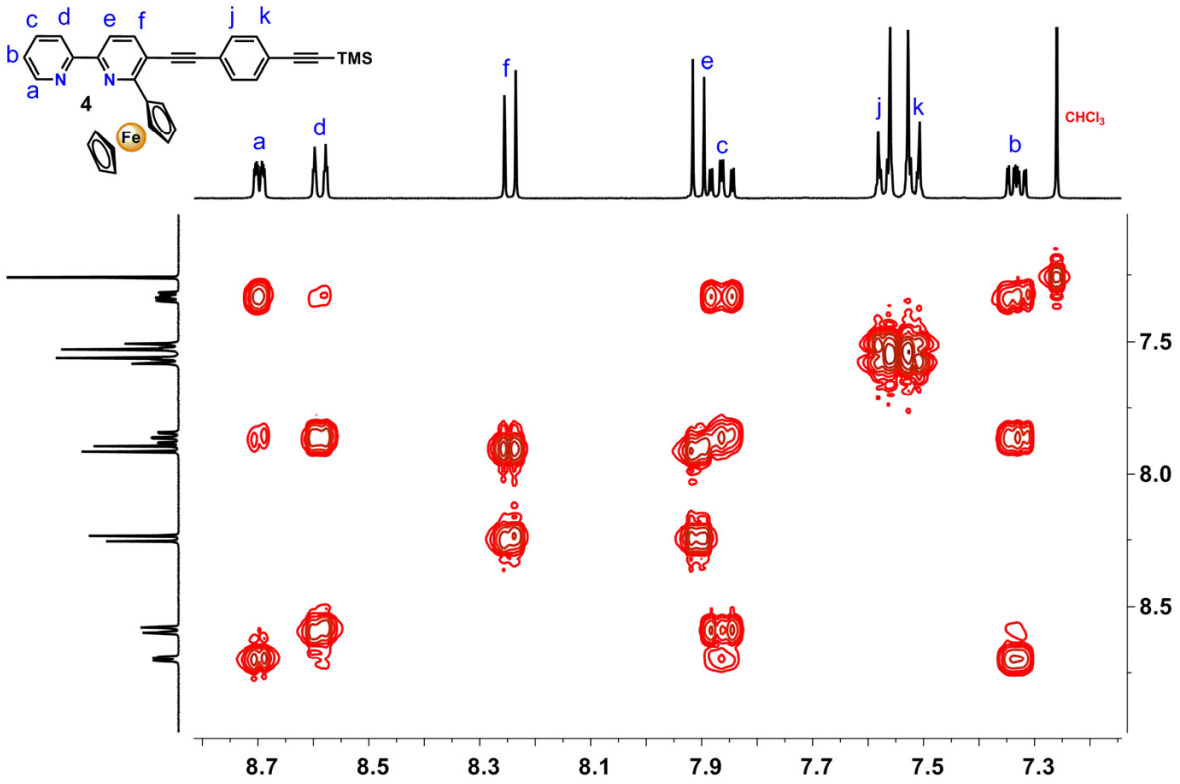

Figure S5. ^{1}H-^{1}H COSY NMR spectrum ($CDCl_3$, 400 MHz, 298 K) of compound **4**.

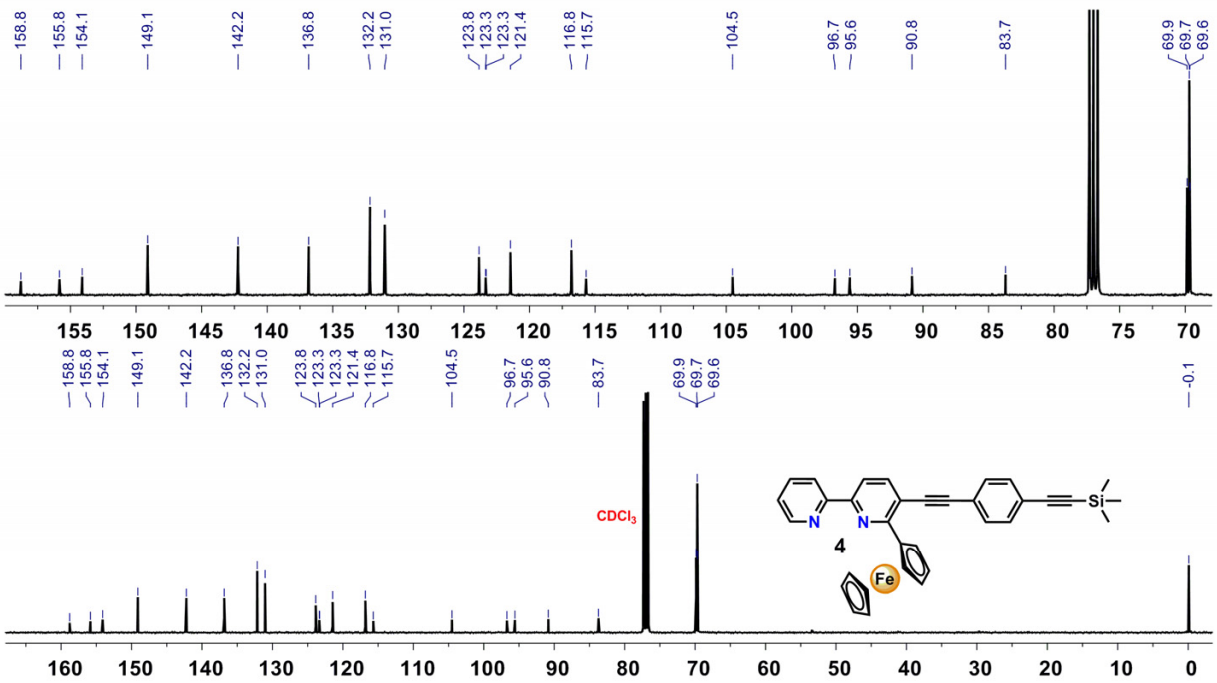

Figure S6. ^{13}C NMR spectrum ($CDCl_3$, 100 MHz, 298 K) of compound **4**.

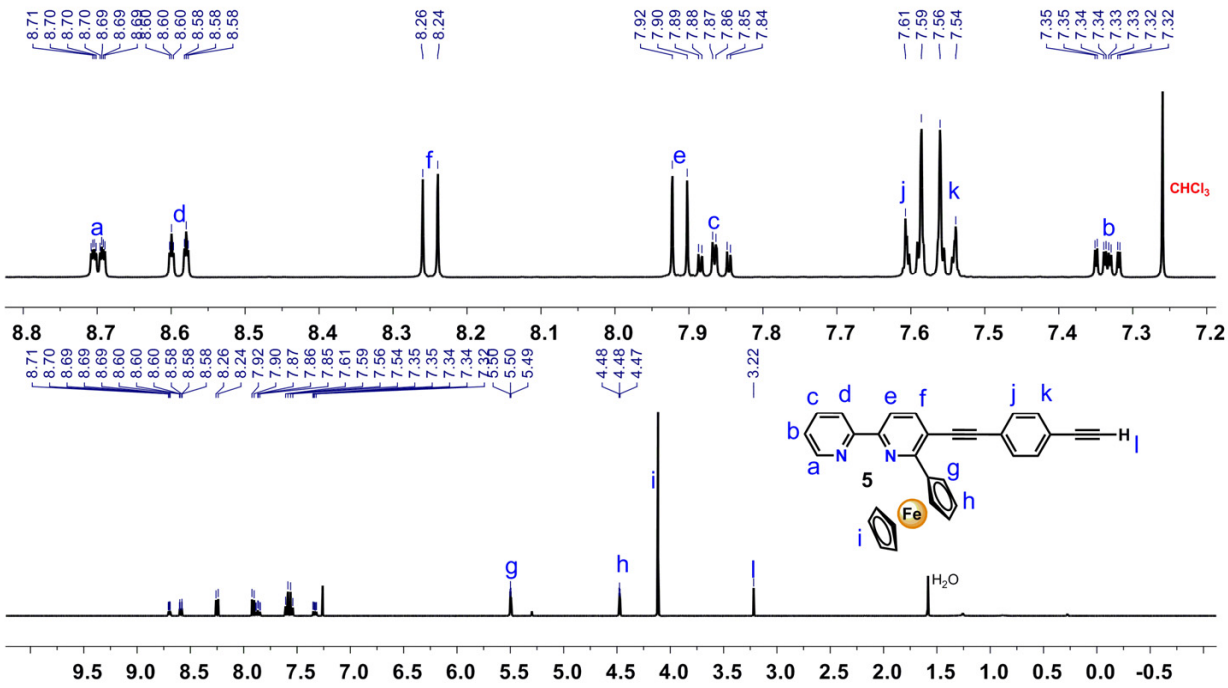

Figure S7. ^{1}H NMR spectrum ($CDCl_3$, 400 MHz, 298 K) of compound **5**.

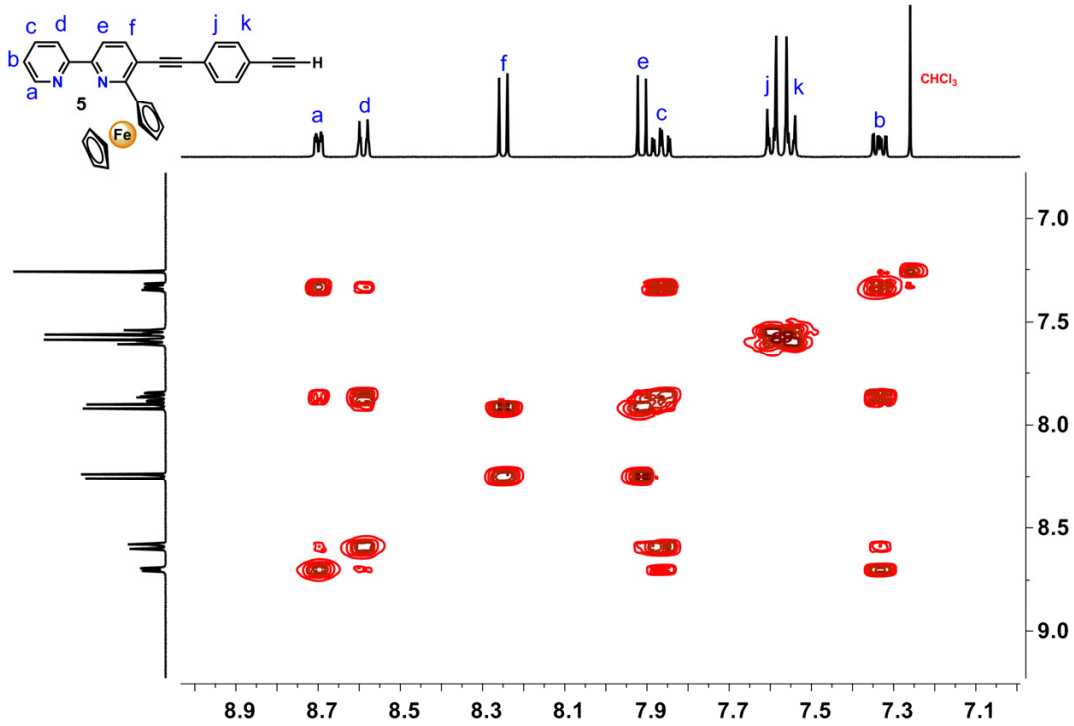

Figure S8. ^{1}H-^{1}H COSY NMR spectrum ($CDCl_3$, 400 MHz, 298 K) of compound **5**.

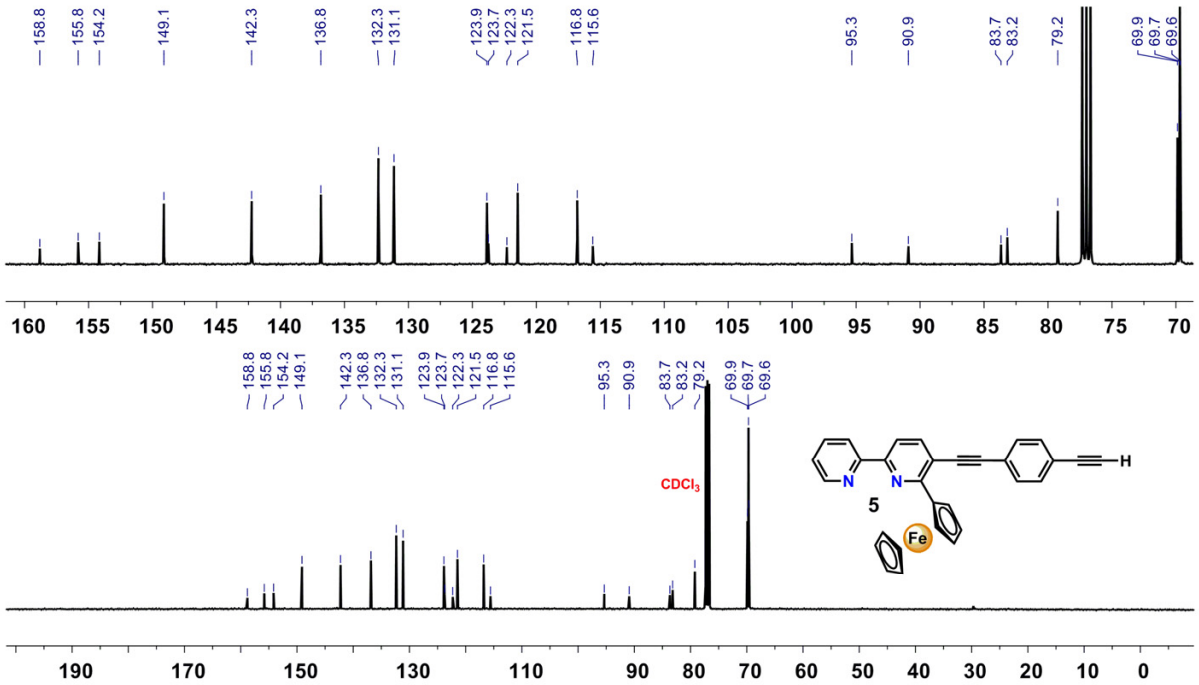

Figure S9. ^{13}C NMR spectrum ($CDCl_3$, 100 MHz, 298 K) of compound **5**.

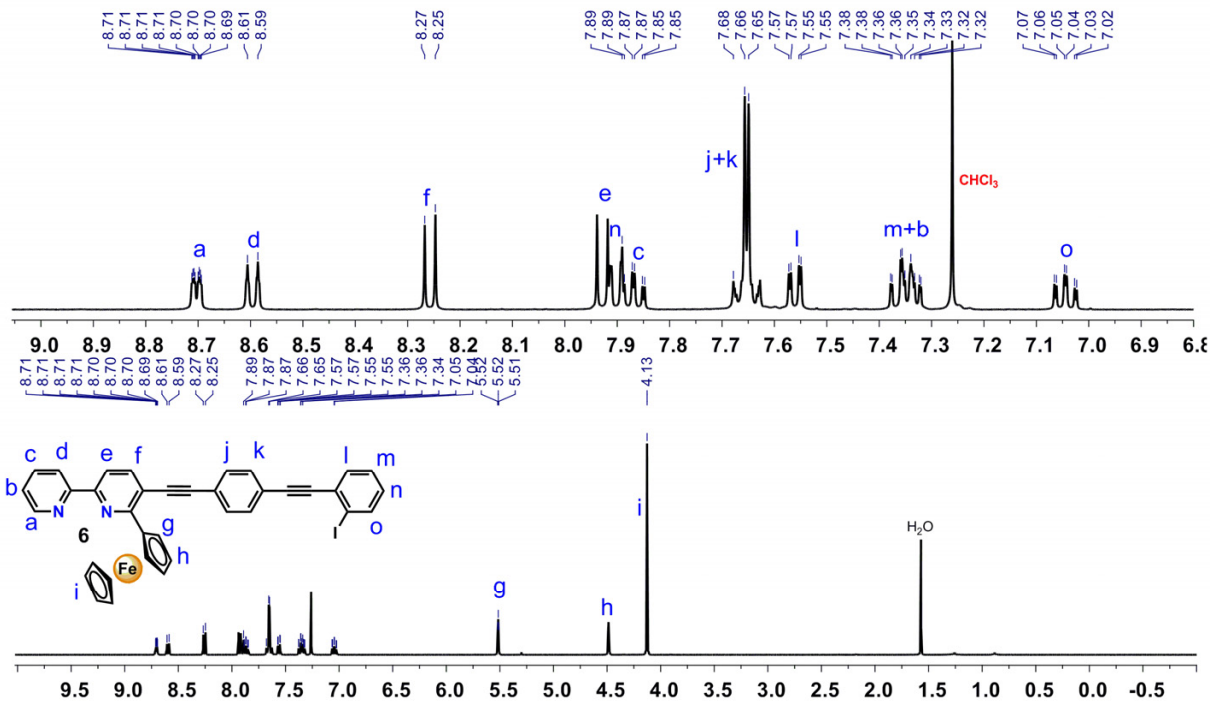

Figure S10. ^{1}H NMR spectrum ($CDCl_3$, 400 MHz, 298 K) of compound **6**.

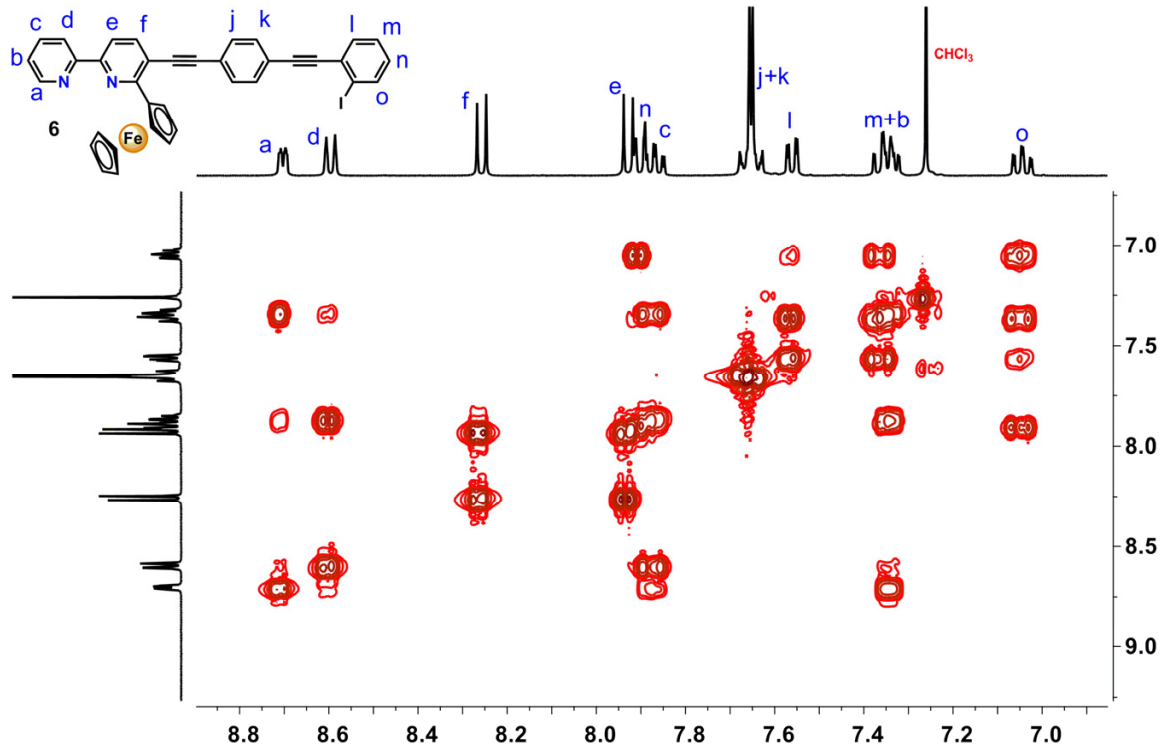

Figure S11. ^{1}H-^{1}H COSY NMR spectrum ($CDCl_3$, 400 MHz, 298 K) of compound **6**.

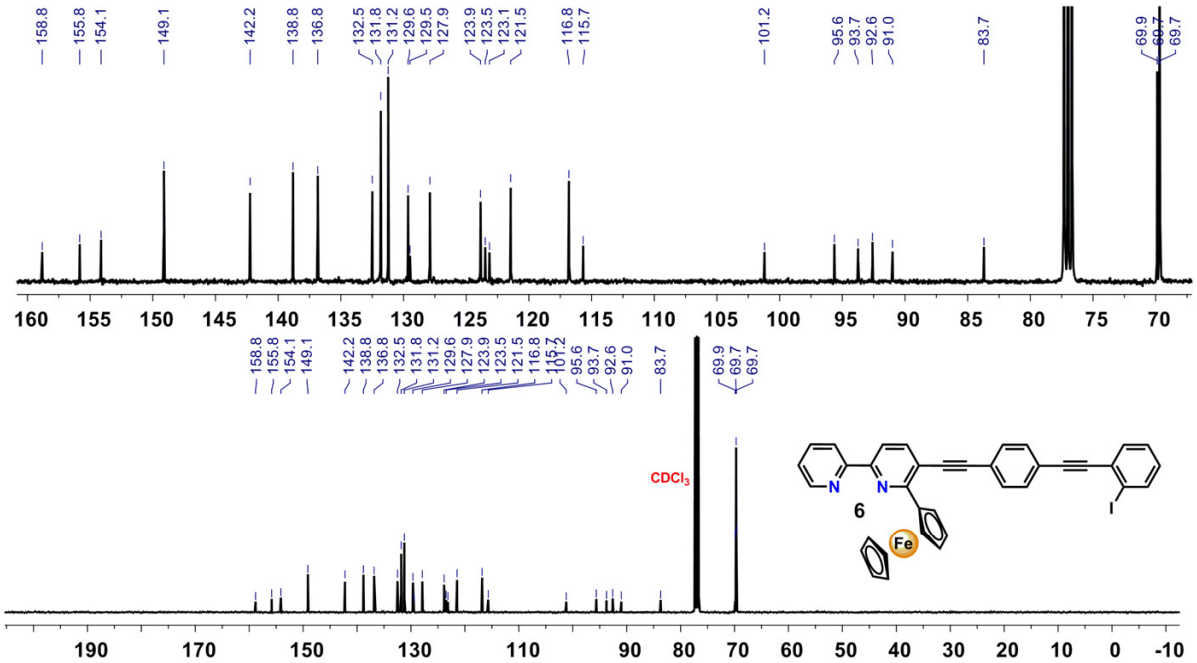

Figure S12. ^{13}C NMR spectrum ($CDCl_3$, 100 MHz, 298 K) of compound **6**.

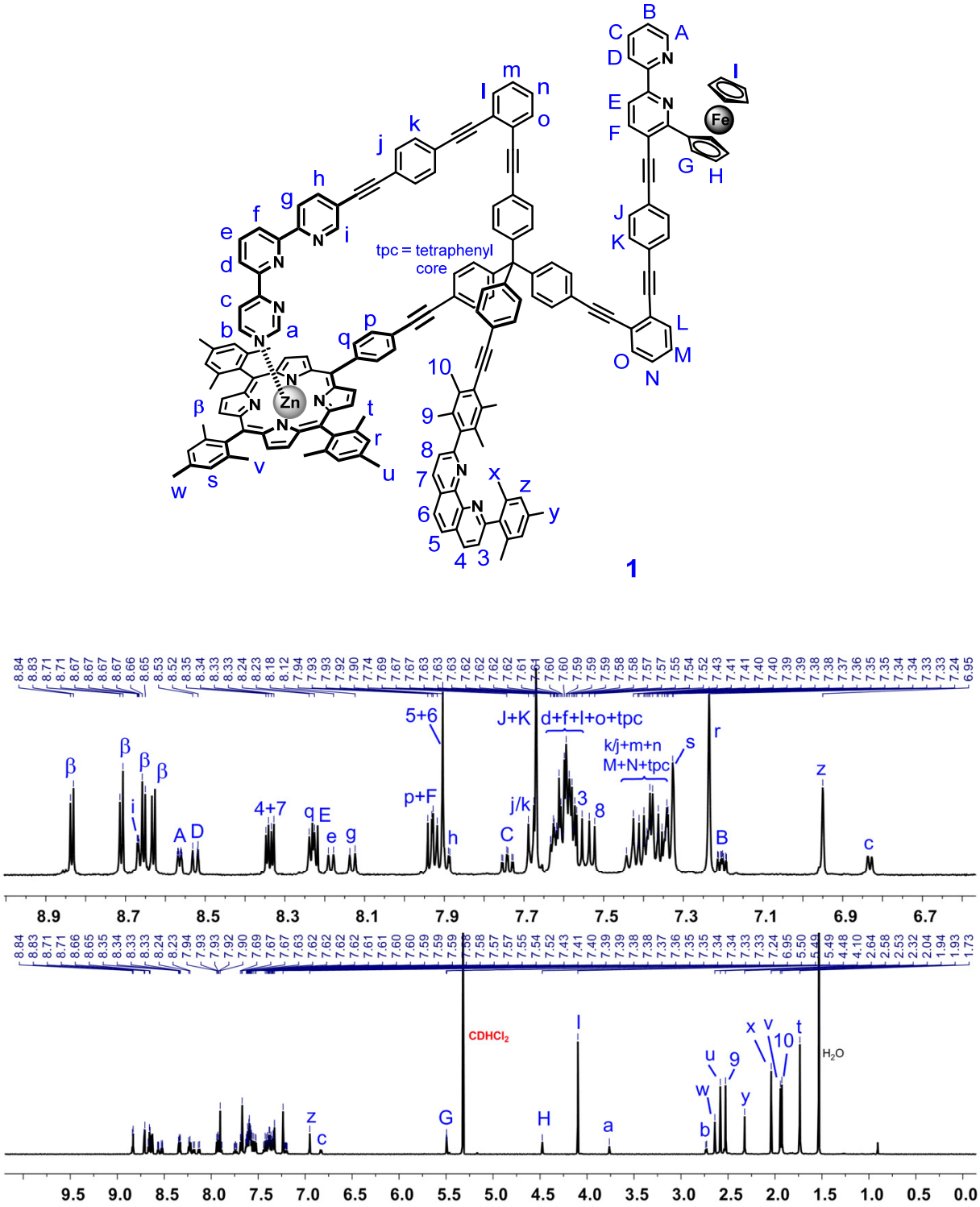

Figure S13. ^{1}H NMR spectrum (CD_2Cl_2, 600 MHz, 298 K) of compound **1**.

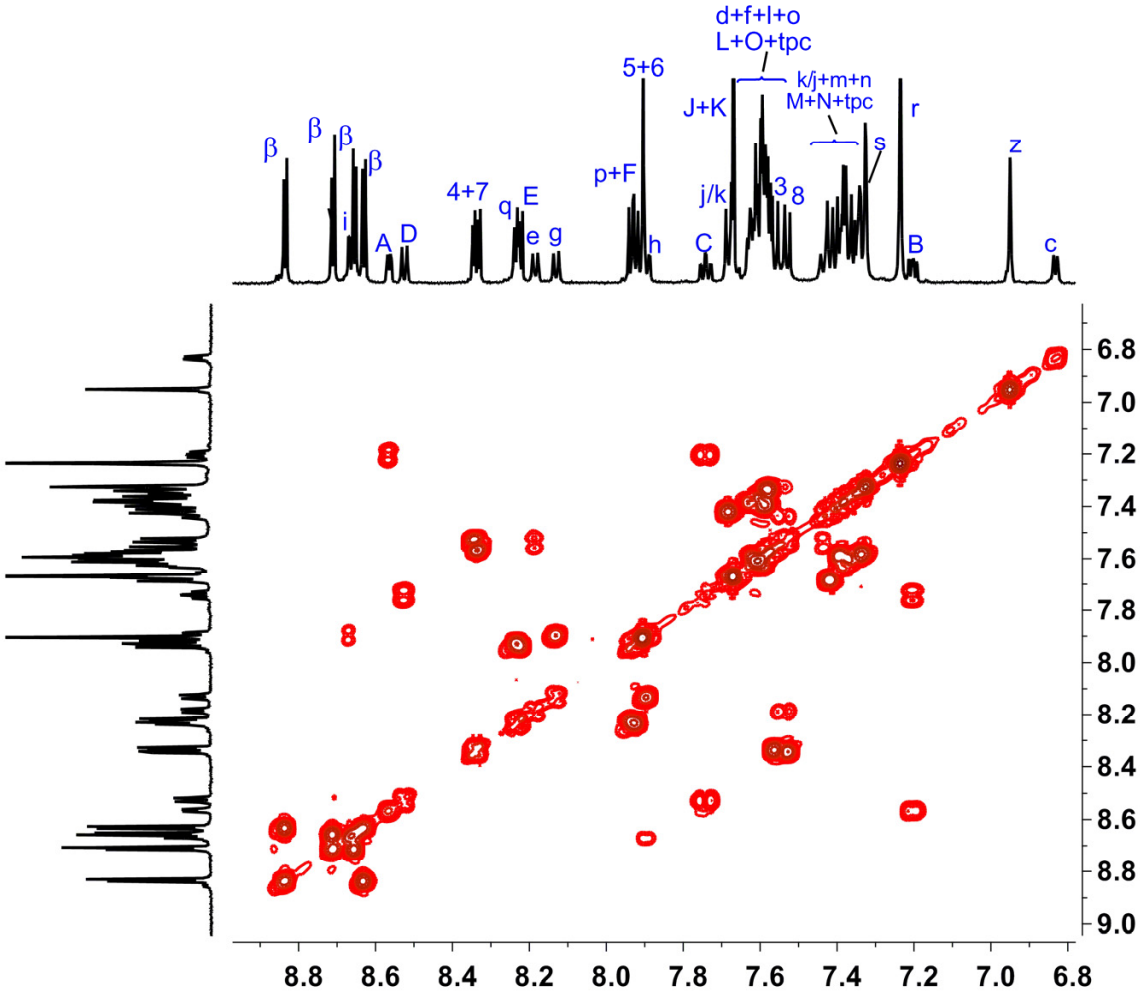

Figure S14. ^{1}H-^{1}H COSY NMR spectrum (CD_2Cl_2, 600 MHz, 298 K) of compound **1**.

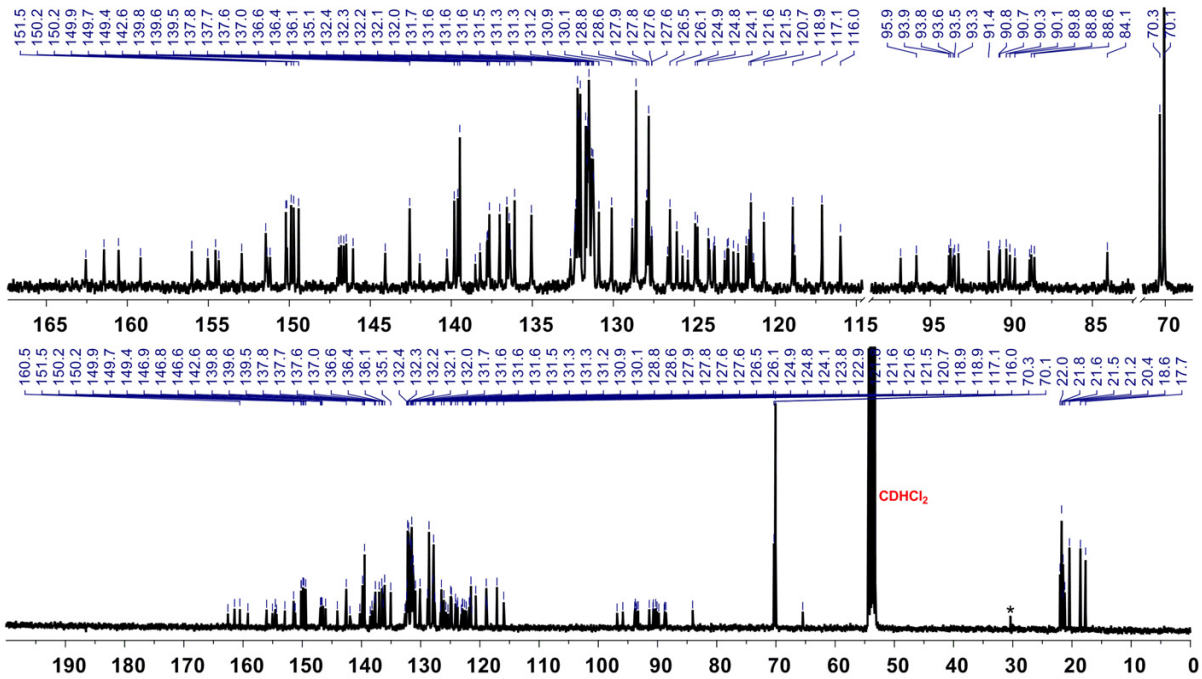

Figure S15. ^{13}C NMR spectrum (CD_2Cl_2, 100 MHz, 298 K) of compound **1**.

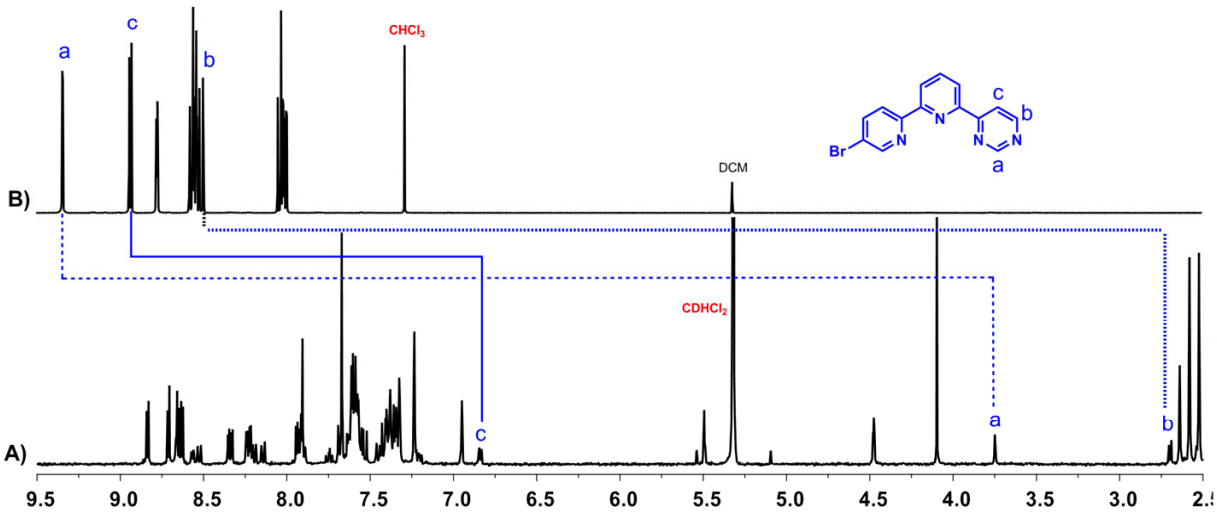

Figure S16. Comparison of partial ^{1}H NMR spectra of A) the bromo-azaterpyridine ($CDCl_3$, 400 MHz, 298 K) and B) nanoswitch **1** (CD_2Cl_2, 400 MHz, 298 K).

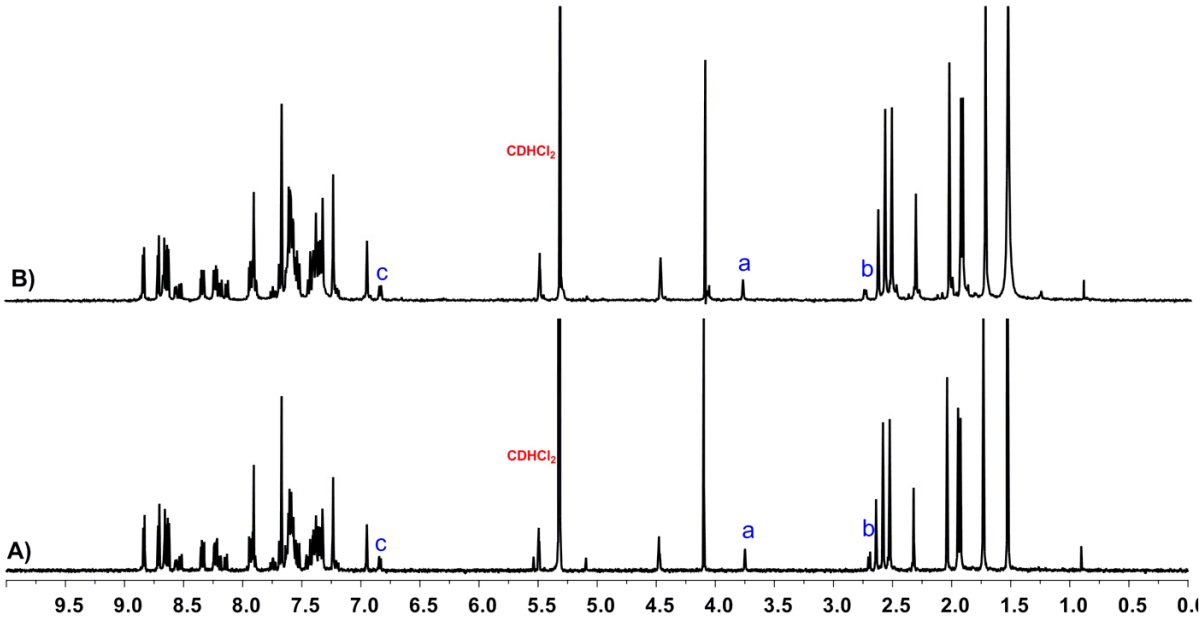

Figure S17. Comparison of partial ^{1}H NMR spectra (CD_2Cl_2, 400 MHz, 298 K) of nanoswitch **1** at two different concentrations: (A) 0.55 mM, and (B) 2.90 mM.

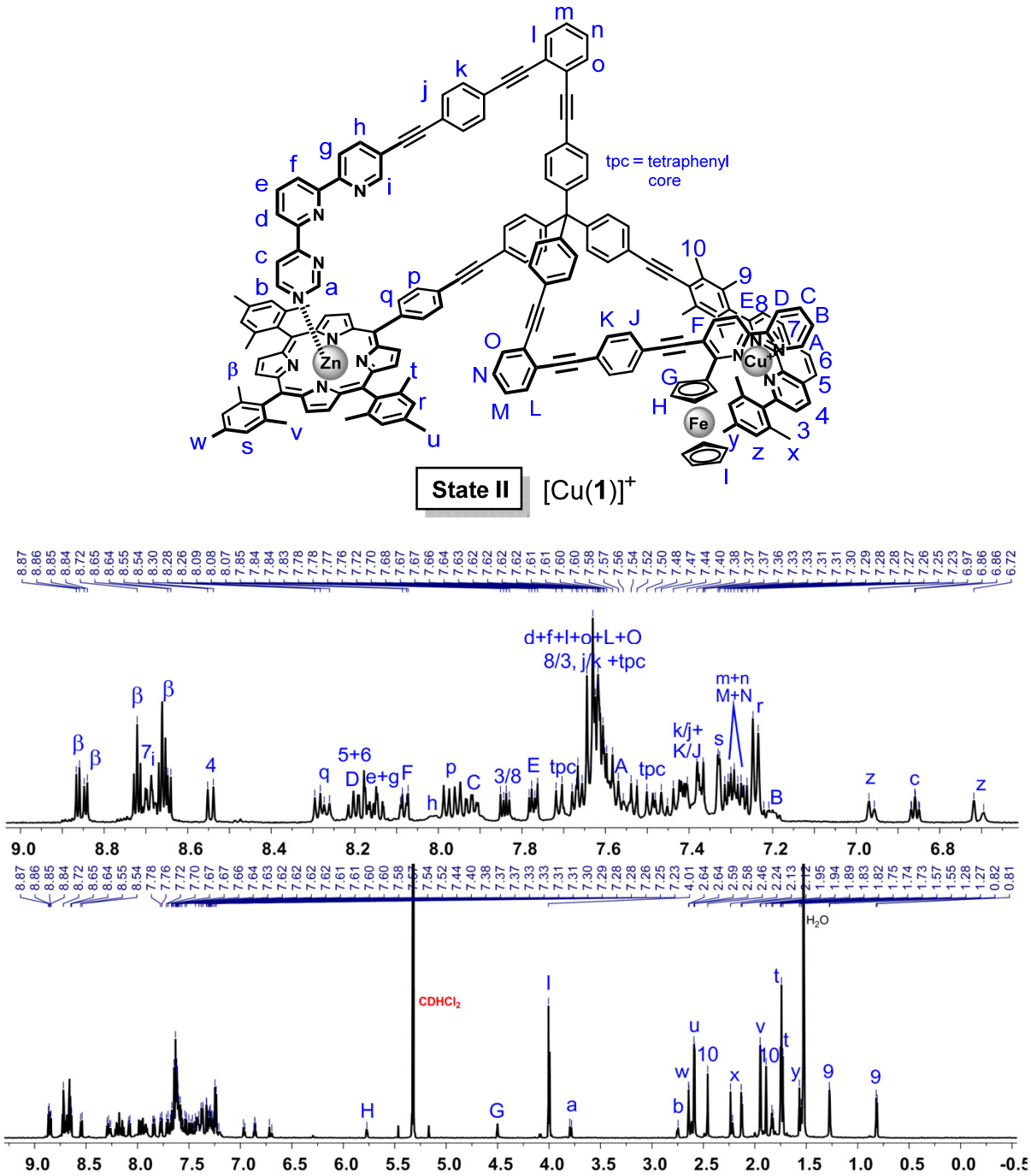

Figure S18. ^{1}H NMR spectrum (CD_2Cl_2, 600 MHz, 298 K) of $[Cu(\mathbf{1})]^+$ complex.

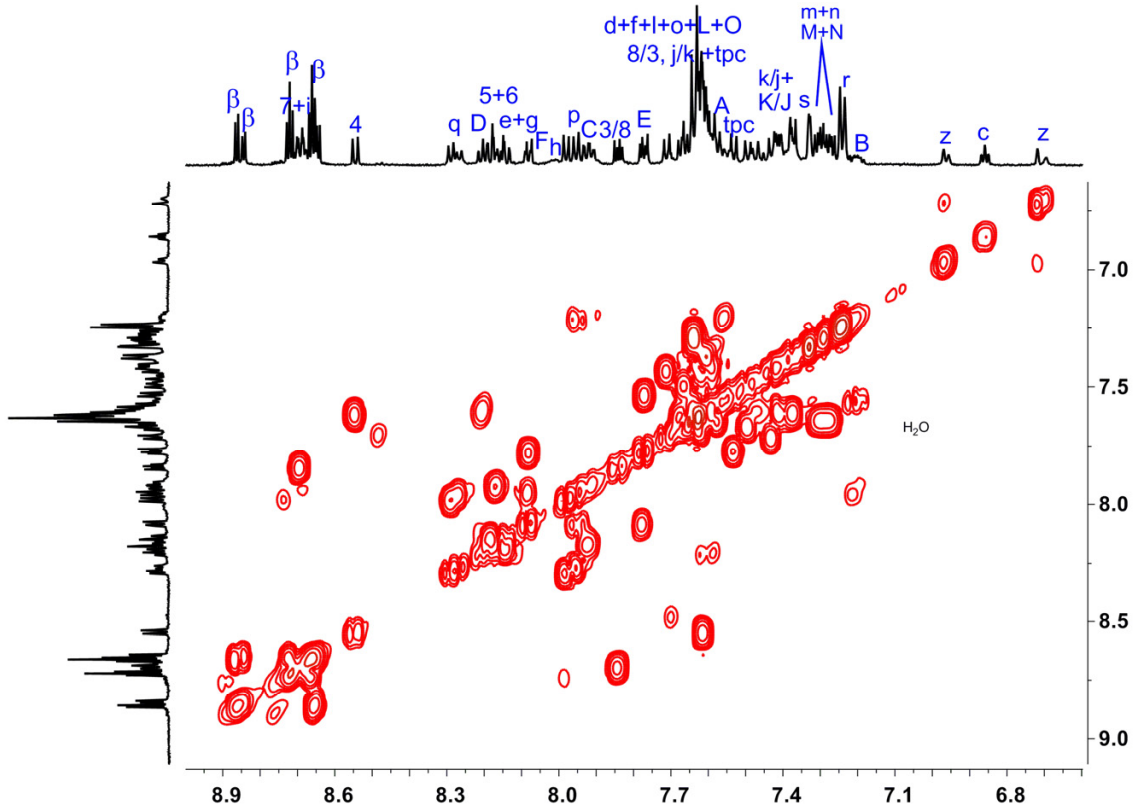

Figure S19. ^{1}H-^{1}H COSY NMR spectrum (CD_2Cl_2, 600 MHz, 298 K) of $[Cu(\mathbf{1})]^{+}$ complex.

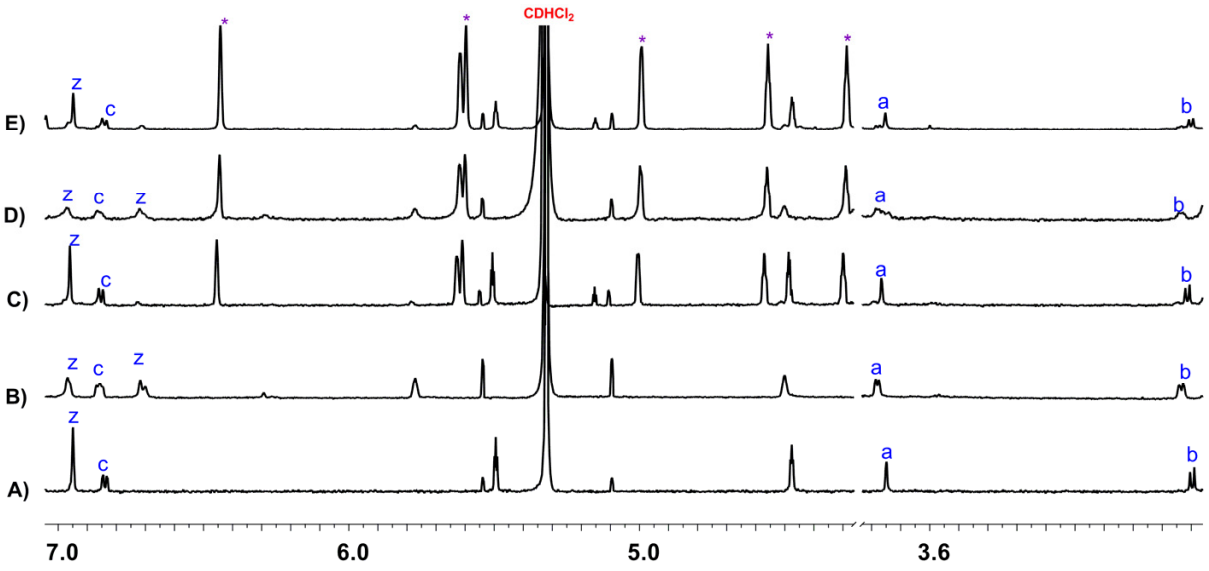

Figure S20. Comparison of partial ^{1}H NMR spectra (CD_2Cl_2, 400 MHz, 298 K) demonstrating the reversibility of switching between states I and II of nanoswitch **1** as realized by successive addition of equimolar amounts of Cu^+ (**B** and **D,** State II) and 2.0 equiv. of 2-ferrocenyl-9-mesityl-[1,10]-phenanthroline (**A**, **C** and **E,** State I). Peaks of the homoleptic copper(I) complex of 2-ferrocenyl-9-mesityl-[1,10]-phenanthroline are indicated by the asterisk.[1]

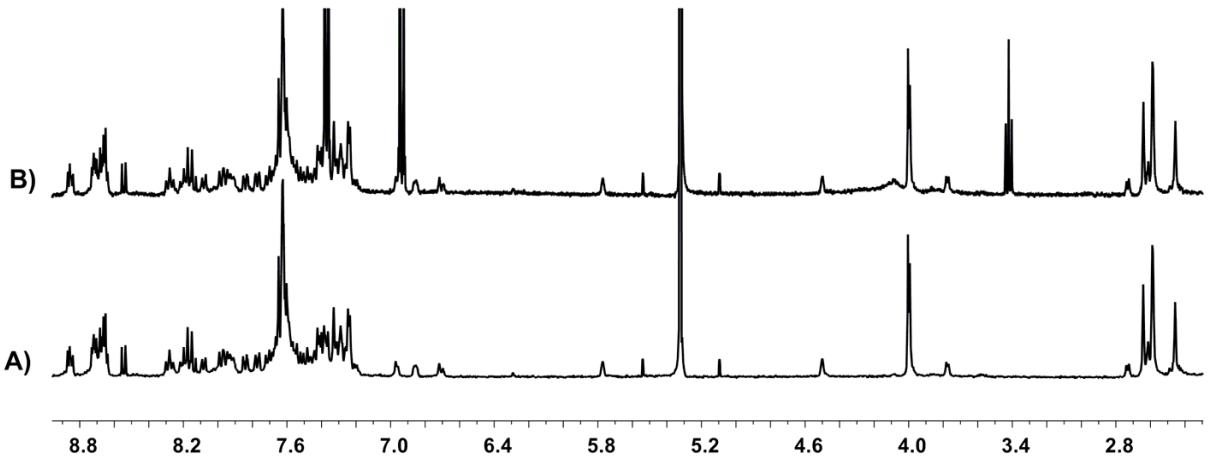

Figure S21. Comparison of partial ^{1}H NMR spectra (CD_2Cl_2, 400 MHz, 298 K) of A) complex $[Cu(\mathbf{1})]^+$ = State II and B) after addition of 1.0 equiv. of $TBA^{+\bullet}BF_4^-$ to the solution of nanoswitch **1**, the reaction mixture was heated at 40 °C for 5 min to ensure the formation of State III, a color change occurred from a greenish purple to orange red confirming detachment of azaterpyridine arm from the ZnPor unit of **1**. Subsequently, the putative solution was reduced by BFD and ^{1}H NMR was measured. The NMR spectrum showed regeneration of State II.

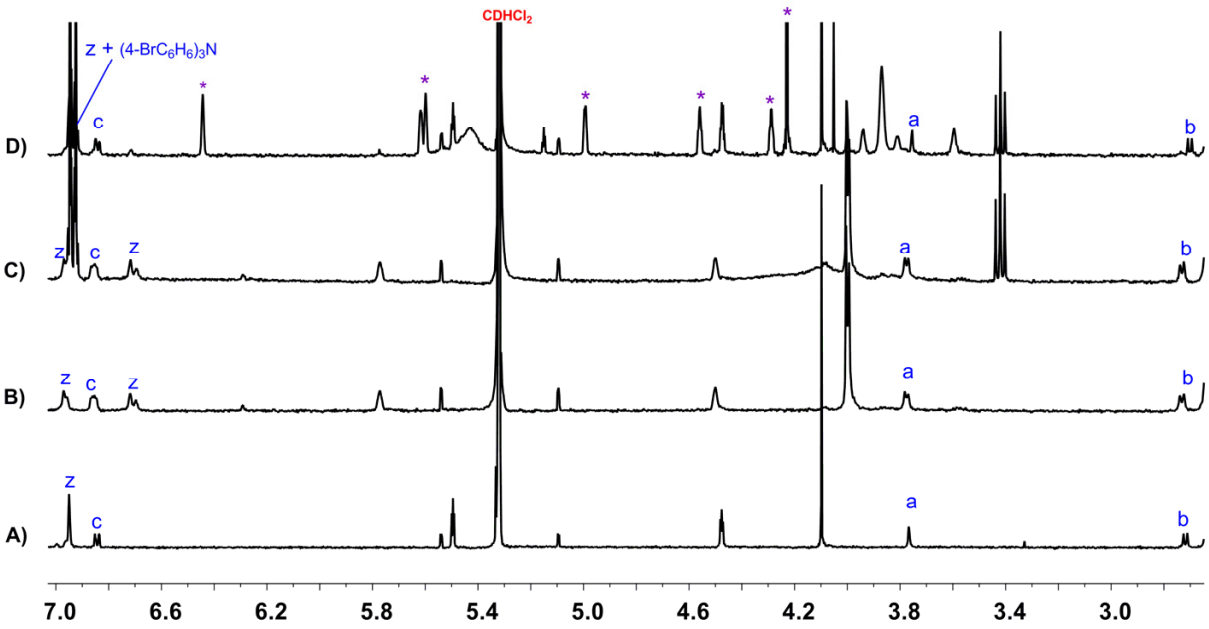

Figure S22. Comparision of partial ^{1}H NMR spectra (CD_2Cl_2, 400 MHz, 298 K) of A) State I (**1**, 960 µg, 0.367 µmol); B) after addition of 1.0 equiv. of ($[Cu(CH_3CN)_4][B(C_6F_5)_4]$ (332 µg, 0.367 µmol) to give $[Cu(\mathbf{1})]^+$ = State II; C) after addition of 1.0 equiv. of $TBA^{+\bullet}BF_4^-$ (209 µg, 0.367 µmol) the reaction mixture was sonicated at 40 °C for 5 min to ensure the formation of State III, a color change occurred from a greenish purple to orange red confirming detachment of the azaterpyridine arm from the ZnPor unit. Subsequently, the putative solution was reduced by 3-(11-bromoundecyl)-1,10-biferrocenylene[2] (BFD, 231 µg, 0.367 µmol) and the ^{1}H NMR was measured. The NMR spectrum showed regeneration of State II; D) 2.0 equiv. of 2-ferrocenyl-9-mesityl-[1,10]-phenanthroline (354 µg, 0.734 µmol) was added and the reaction mixture was heated at 40 °C to reset to State I. Peaks of the homoleptic copper(I) complex of 2-ferrocenyl-9-mesityl-[1,10]-phenanthroline are indicated by the asterisk.

2. UV-vis spectra

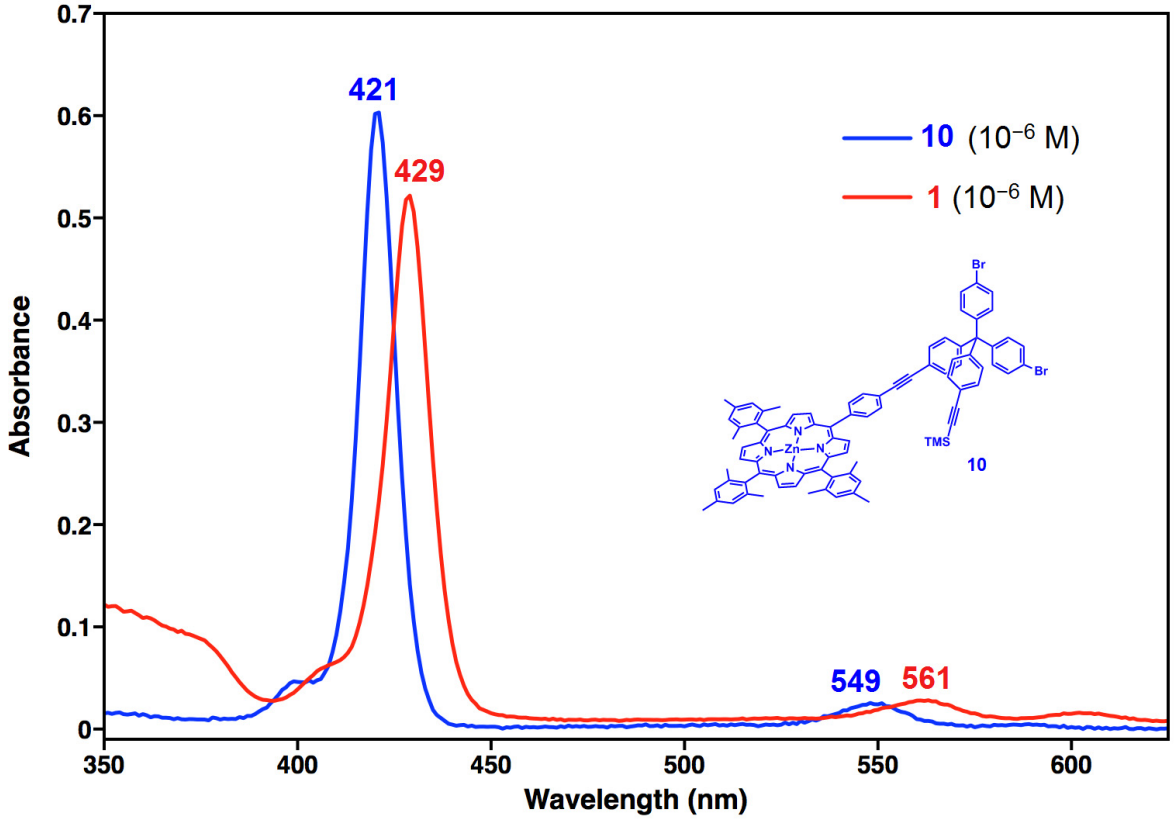

Figure S23. UV-vis spectra of uncoordinated ZnTPP compound **10** (10^{-6} M) and nanoswitch **1** (10^{-6} M) in dichloromethane at 298 K.

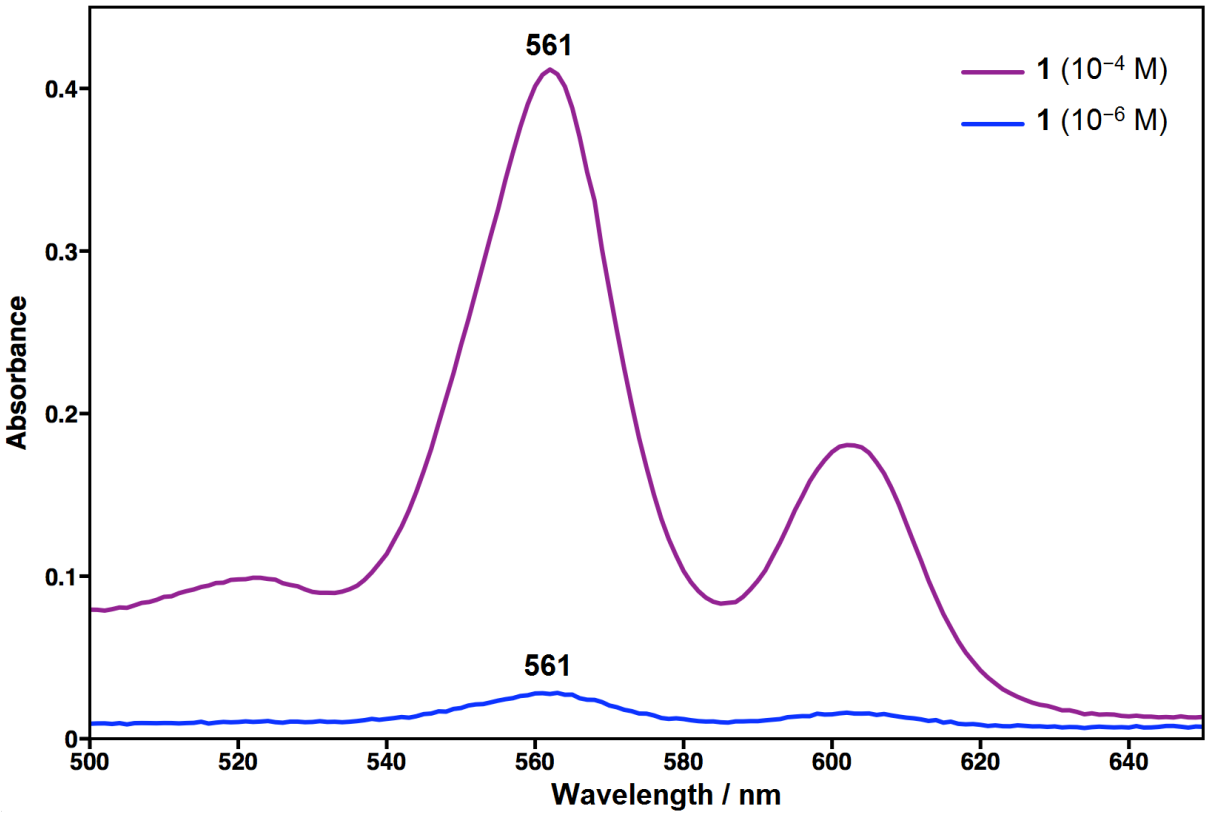

Figure S24. UV-vis spectra of nanoswitch **1** at 10^{-4} M and 10^{-6} M in dichloromethane at 298 K.

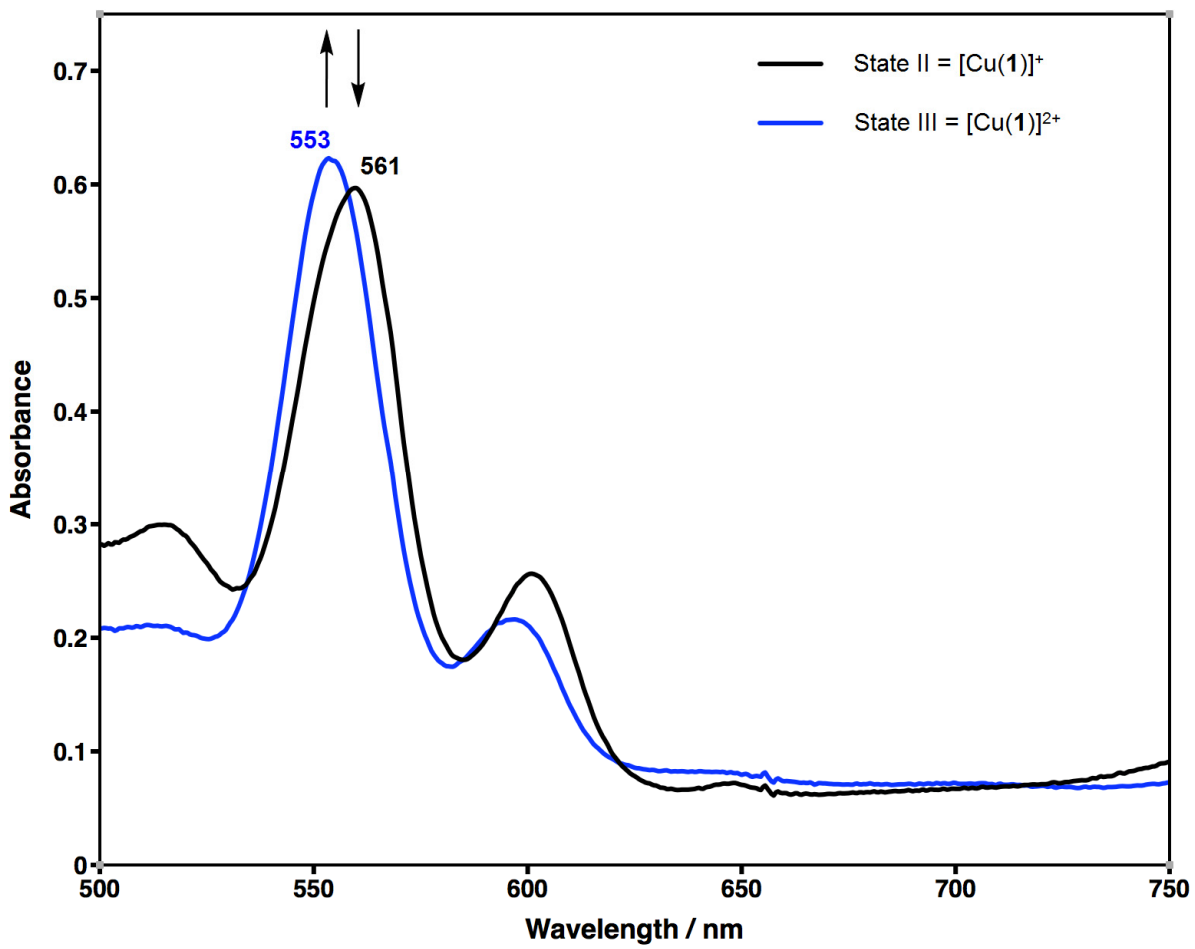

Figure S25. UV-vis spectra of State II = $[Cu(\mathbf{1})]^{+}$ (2×10^{-4} M) and State III = $[Cu(\mathbf{1})]^{2+}$ (2×10^{-4} M) in dichloromethane at 298 K.

After addition of 1.0 equiv. of $TBA^{+\bullet}$ to solution of State II (= $[Cu(\mathbf{1})]^{+}$) in dichloromethane, the Q-band at 561 nm shifted to 553 nm within 12 min at room temperature confirming a swing of the azaterpyridine rotary arm from the ZnPor to the copper(I)-loaded phenanthroline station.

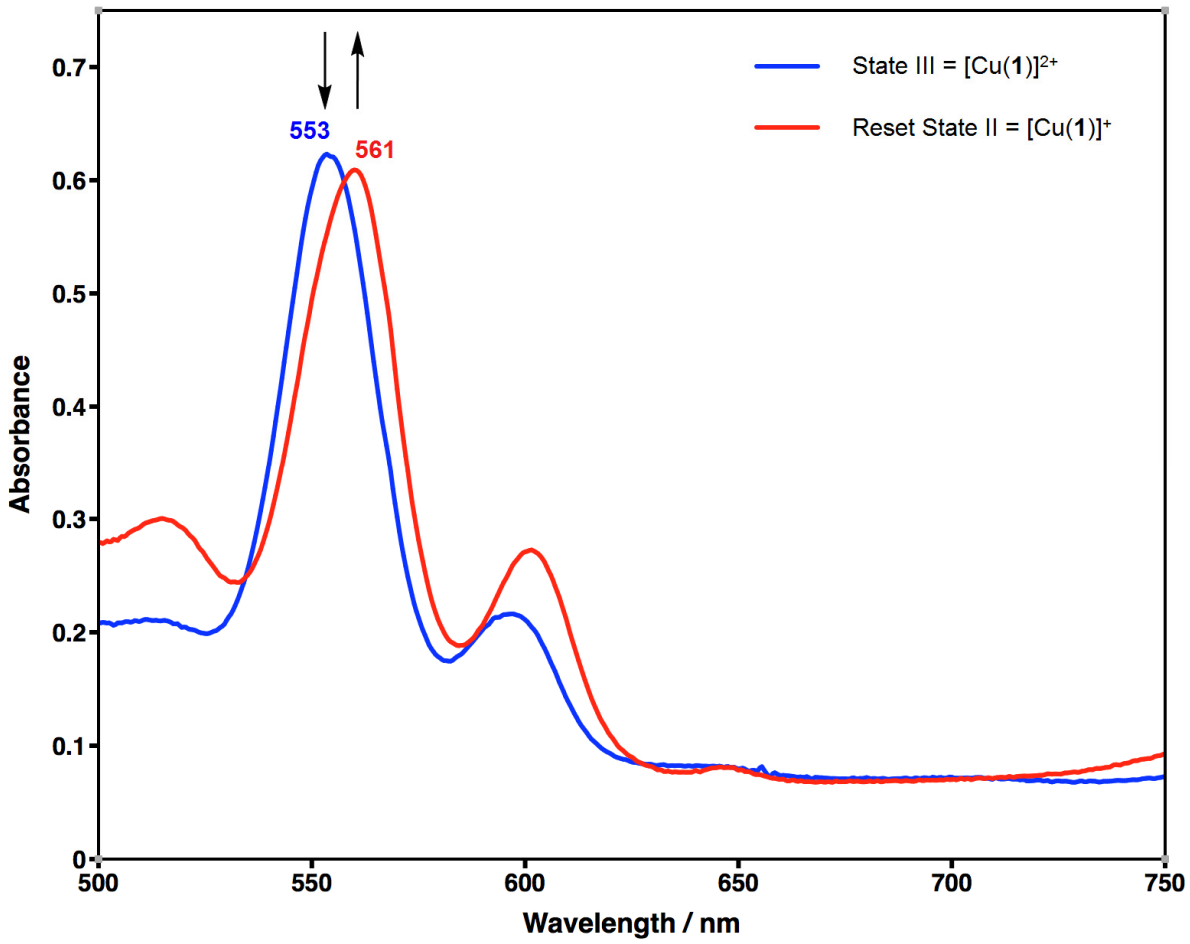

Figure S26. UV-vis spectra of State III = $[Cu(\mathbf{1})]^{2+}$ (2×10^{-4} M) and reset of State II = $[Cu(\mathbf{1})]^{+}$ (2×10^{-4} M) in dichloromethane at 298 K.

After addition of 1.0 equiv. of dmfc to solution of State III (= $[Cu(\mathbf{1})]^{2+}$) in dichloromethane, the Q-band at 553 nm shifted to 561 nm within 1 min at room temperature attesting relocation of the azaterpyridine arm from the copper(I)-loaded phenanthroline to the ZnPor station.

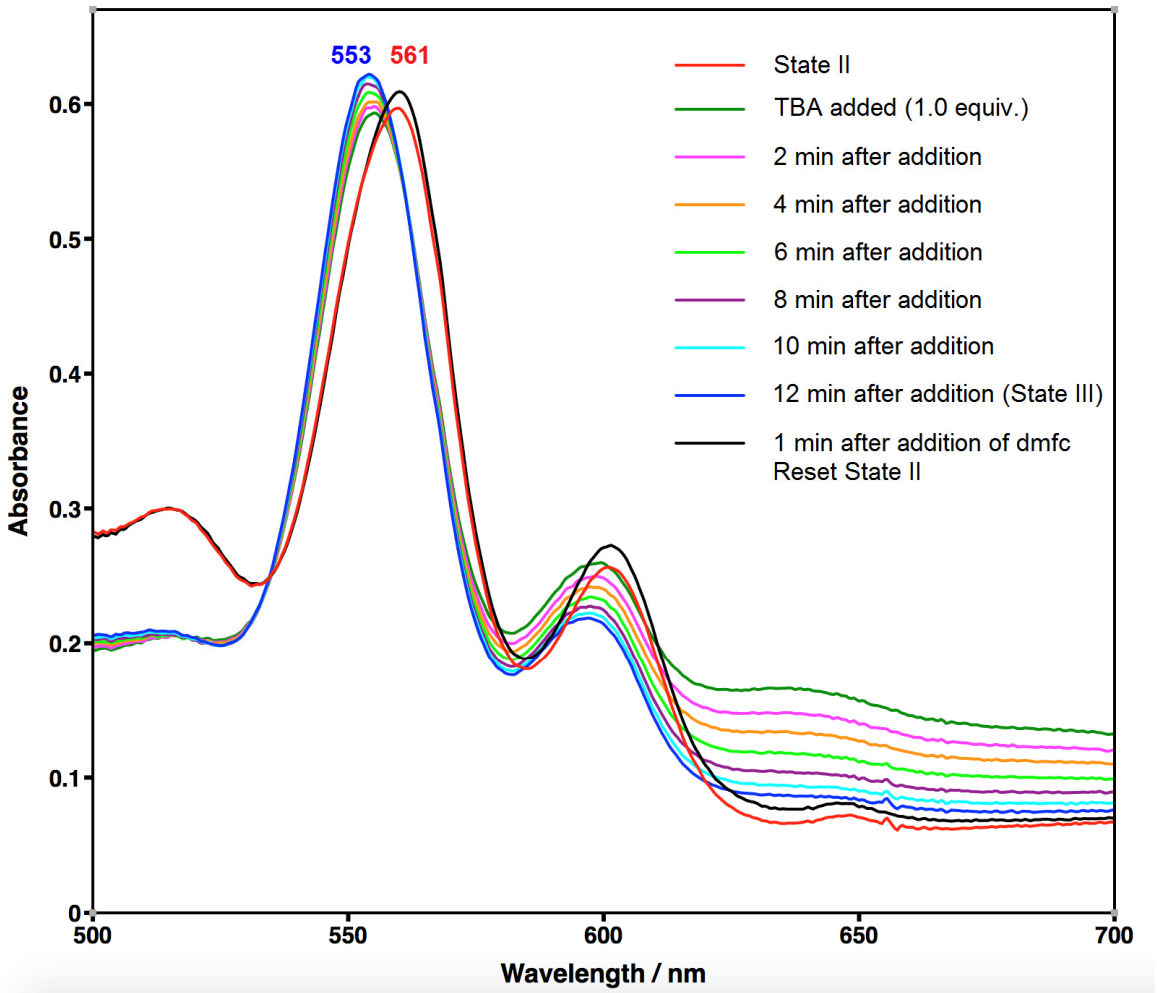

Figure S27. UV-vis spectra showing reversible switching between State II and State III of the nanoswitch **1**.

A mixture of nanoswitch **1** (262 µg, 0.100 µmol) and 1.0 equiv. of $[Cu(CH_3CN)_4][B(C_6F_5)_4]$ (91 µg, 0.100 µmol) was dissolved in dichloromethane (500 µl, $c = 2 \times 10^{-4}$ M) to afford State II (= $[Cu(\mathbf{1})]^+$, red trace). The UV-vis spectrum displays an absorption at 561 nm (Q-band). After treatment with 1.0 equiv. of $TBA^{+\bullet}$ (82 µg, 0.100 µmol), the Q-band shifted to 553 nm within 12 min (blue trace) at room temperature. After reduction of State III with 1.0 equiv. of dmfc (33 µg, 0.100 µmol), the Q-band shifted back to 561 nm within 1 min at room temperature (black trace) suggesting formation of State II.

3. ESI-MS spectra

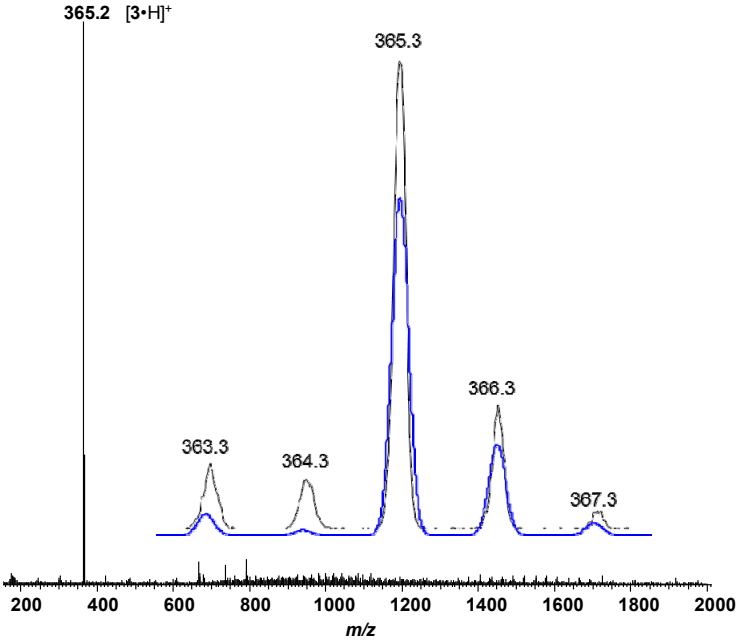

Figure S28. ESI-MS spectrum of compound **3** in dichloromethane after protonation.

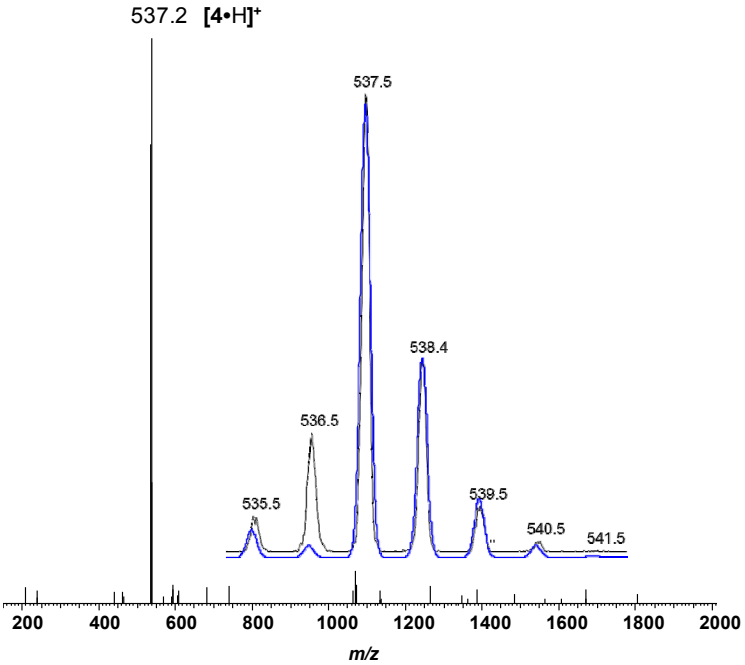

Figure S29. ESI-MS spectrum of compound **4** in dichloromethane after protonation.

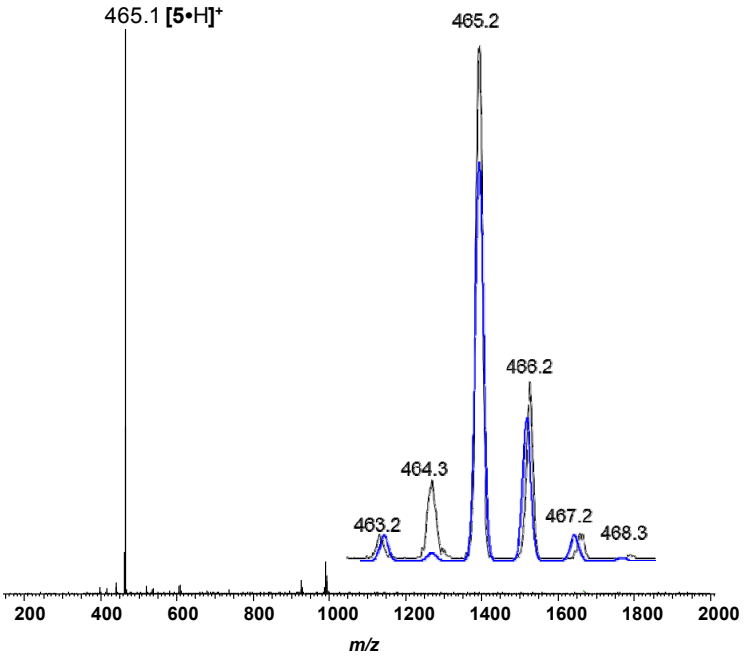

Figure S30. ESI-MS spectrum of compound **5** in dichloromethane after protonation.

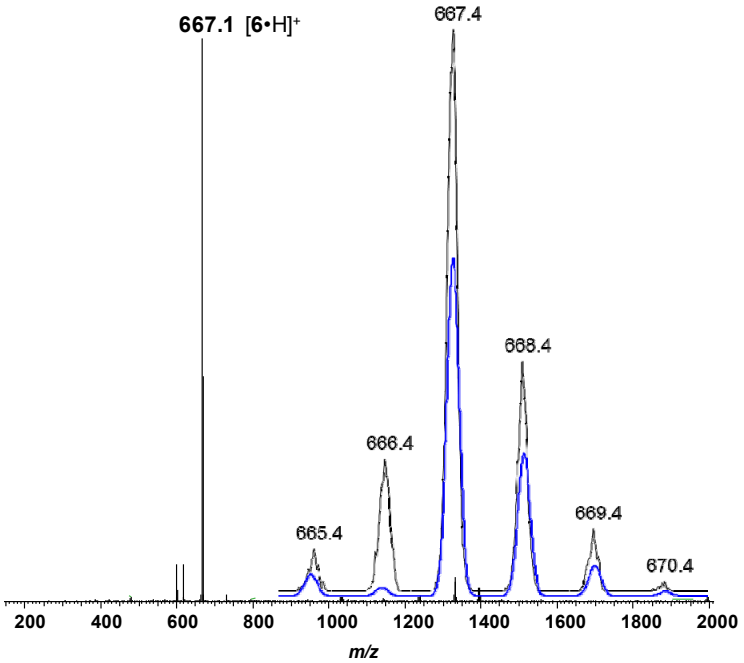

Figure S31. ESI-MS spectrum of compound **6** in dichloromethane after protonation.

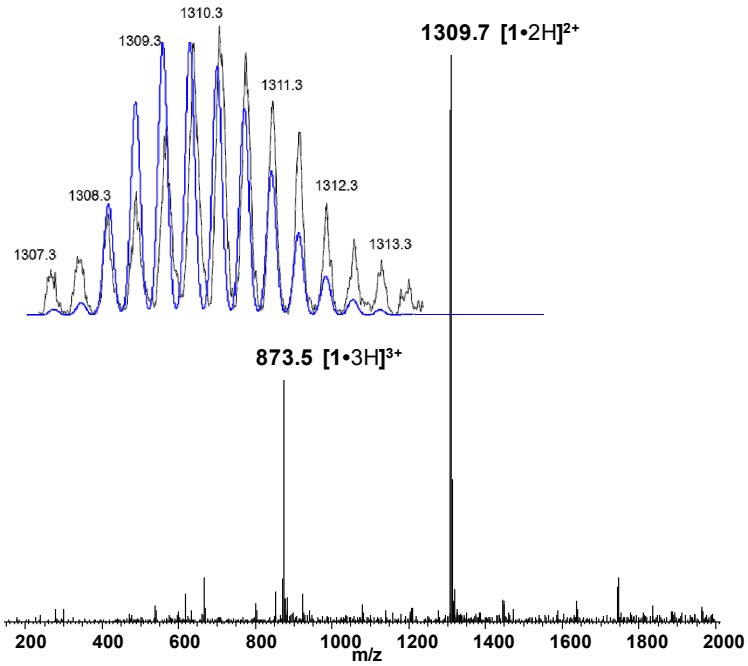

Figure S32. ESI-MS spectrum of compound **1** in dichloromethane after protonation.

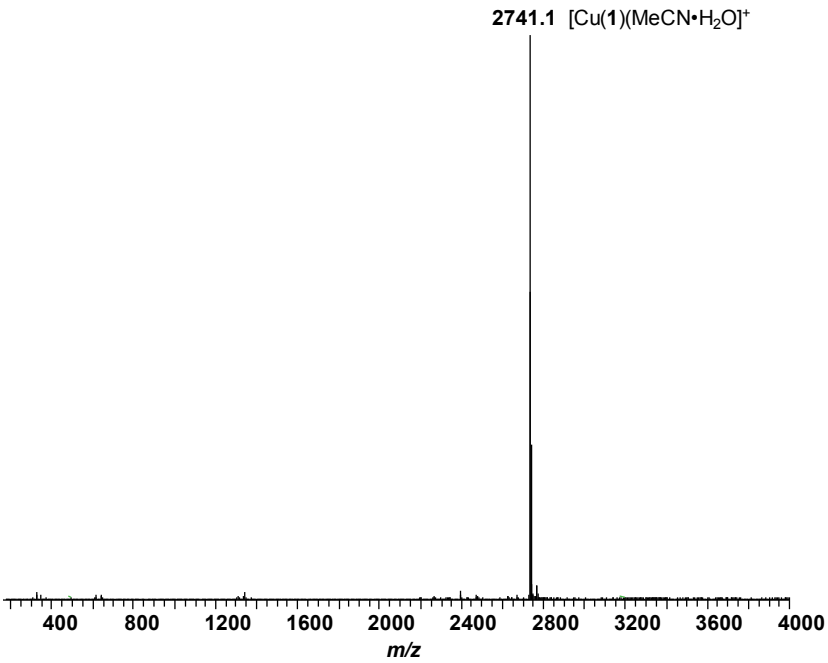

Figure S33. ESI-MS spectrum of complex **1** (State II = $[Cu(\mathbf{1})]^{+}$) in dichloromethane.

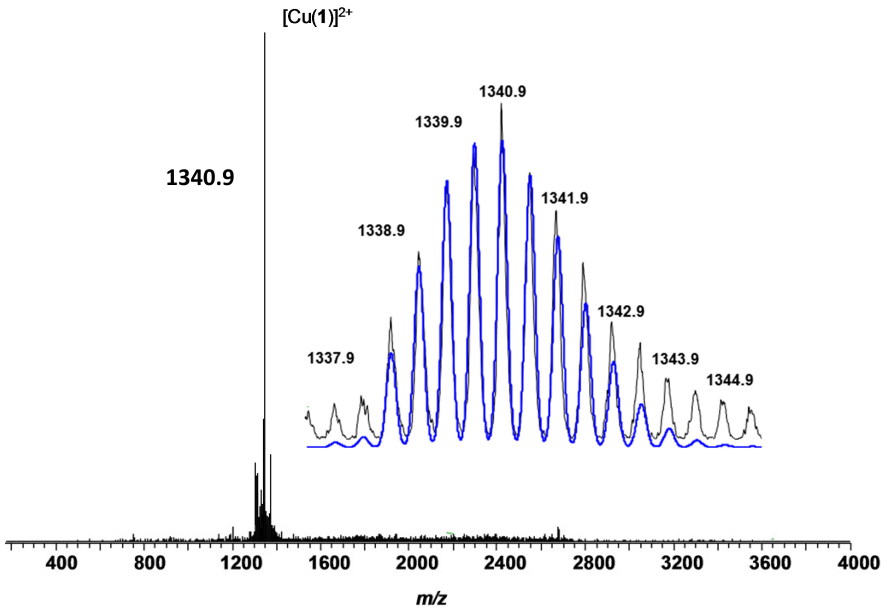

Figure S34. ESI-MS spectrum obtained after oxidation of State II = $[Cu(\mathbf{1})]^{+}$ by $TBA^{+\bullet}$ in dichloromethane.

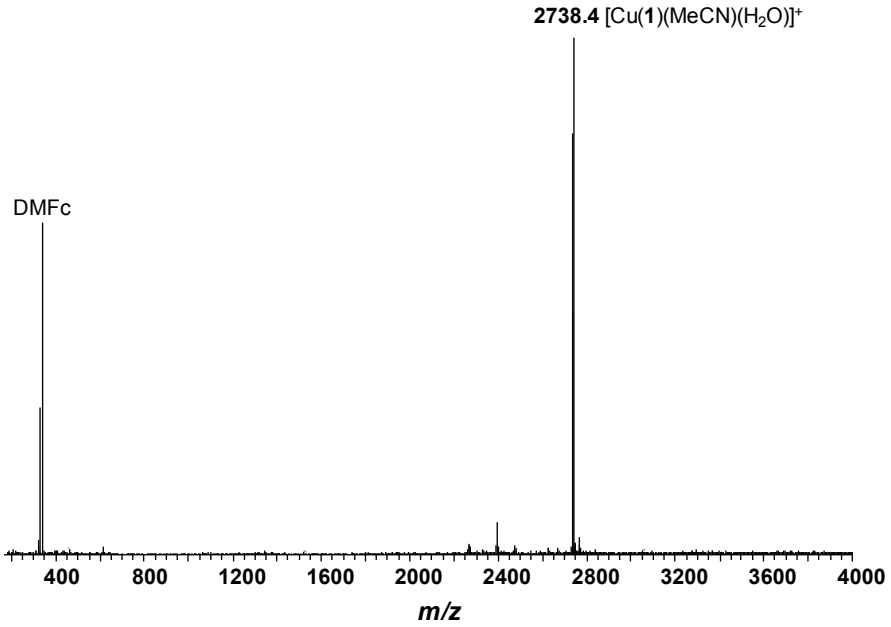

Figure S35. ESI-MS spectrum obtained after reduction of State III = $[Cu(\mathbf{1})]^{2+}$ (solution from Figure S34) by dmfc in dichloromethane.

4. Cyclic voltammetry

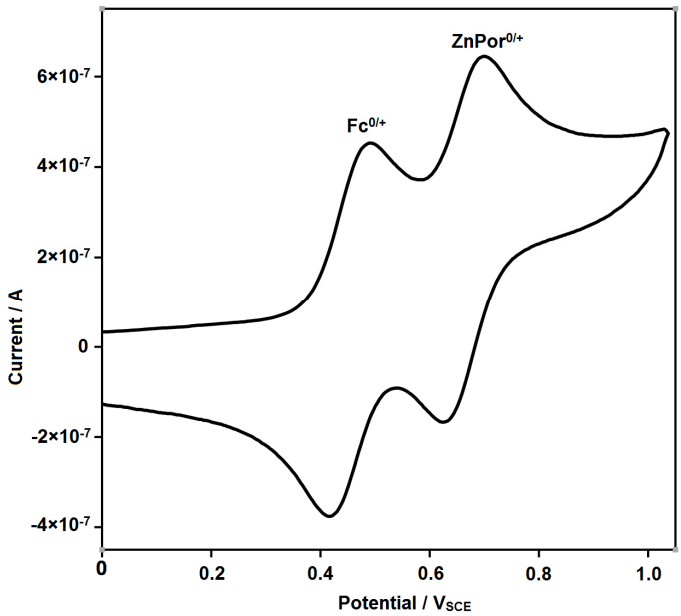

Figure S36. CV of nanoswitch **1** (scan rate of 100 mVs^{-1}) in dry dichloromethane: $Fc^{0/+}$ at $E_{1/2}$ = 0.45 V_{SCE} and ZnPor $^{0/+}$ at $E_{1/2}$ = 0.66 V_{SCE}.

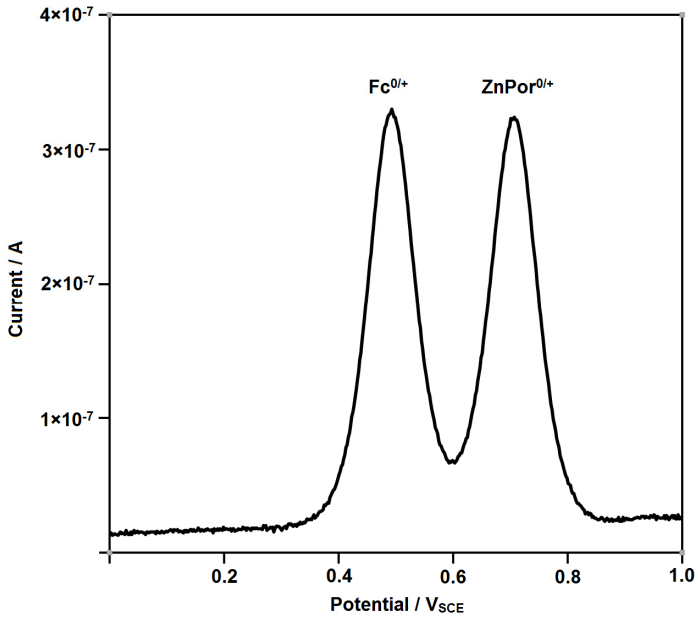

Figure S37. DPV study of nanoswitch **1** in dry dichloromethane (scan rate of 20 mVs^{-1} and a pulse height of 2 mV).

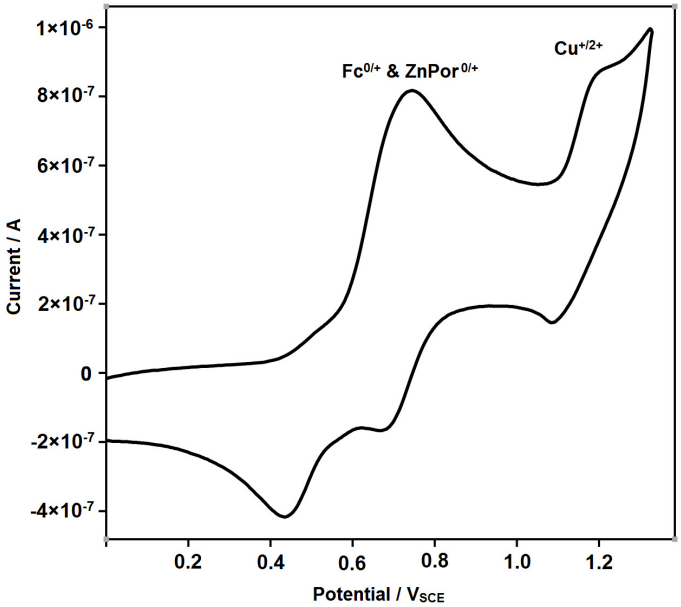

Figure S38. CV of complex $[Cu(\mathbf{1})]^+$ in dry dichloromethane (scan rate of 100 mV s^{-1}).

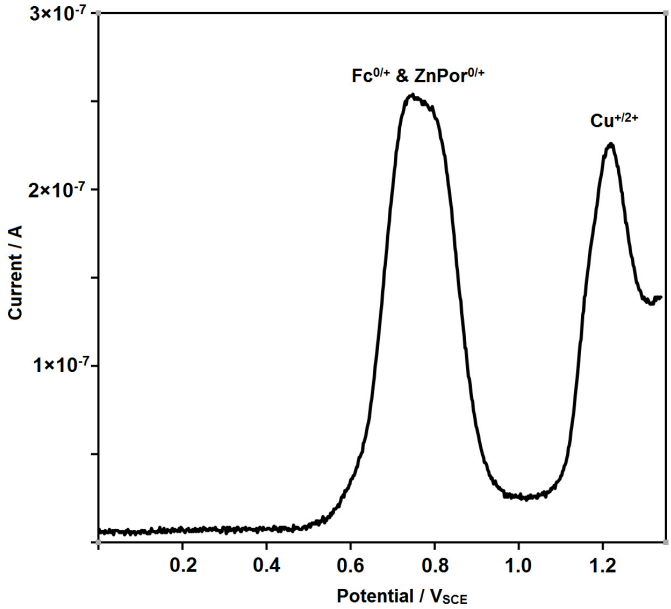

Figure S39. DPV study of complex $[Cu(\mathbf{1})]^+$ in dry dichloromethane (scan rate = 20 mVs^{-1} and pulse height = 2 mV). $Fc^{0/+}$ at $E_{1/2}$ = 0.74 V_{SCE}, $ZnPor^{0/+}$ at $E_{1/2}$ = 0.78 V_{SCE} and $Cu^{+/2+}$ at $E_{1/2}$ = 1.22 V_{SCE}.

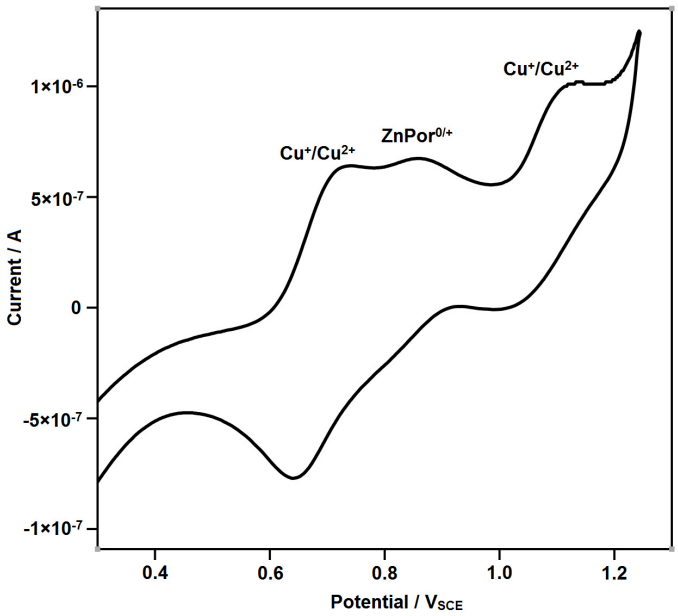

Figure S40. CV of complex $[Cu(\mathbf{1})]^+$ in dry dichloromethane (scan rate of 100 mV s^{-1}) after chemical oxidation with 1.0 equiv. of $TBA^{+\bullet}$: $Cu^{+/2+}$ shows up in two coordination scenarios at $E_{1/2}$ = 0.69 and at 1.10 V_{SCE}. The scan was started 5 min after mixing.

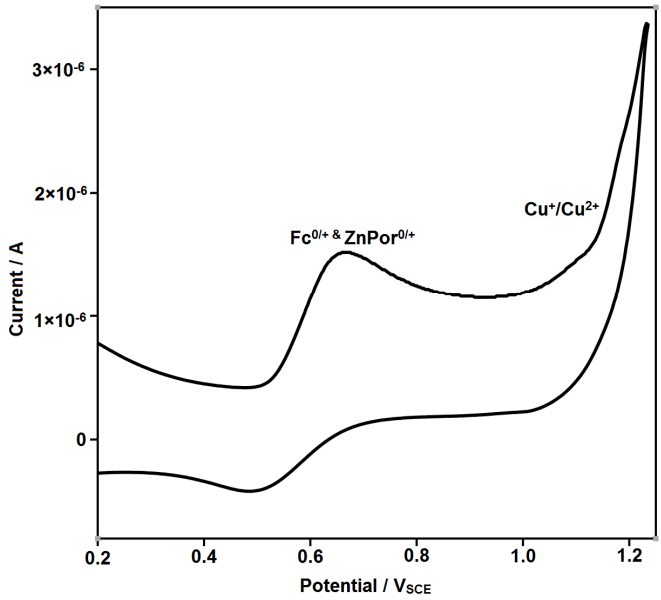

Figure S41. CV of the mixture of **1**, Cu^+ and $TBA^{+\bullet}$ (solution from Figure S40) after reduction with one equiv. of dmfc.

5. Binding Constants

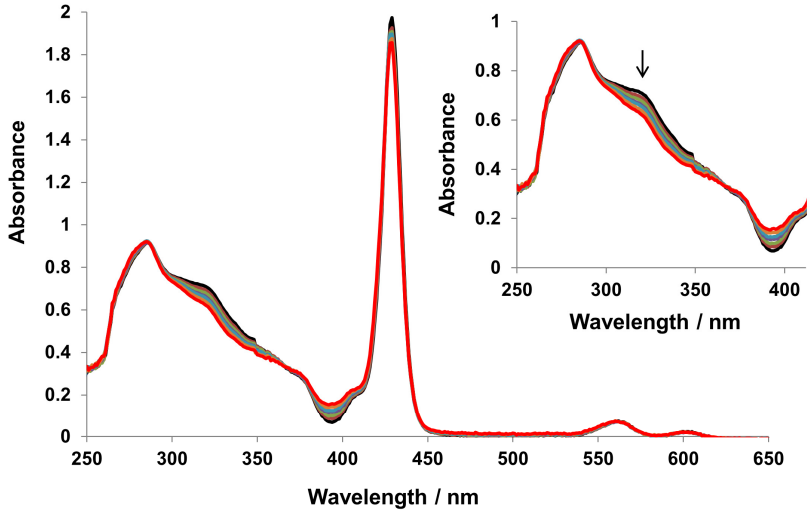

Figure S42. UV-vis spectra of switch **1** (2.5×10^{-5} M) in $CHCl_3$ (0.5 mL) upon addition of $[Cu(CH_3CN)_4]B(C_6F_5)_4$ (1.2×10^{-4} M) at 298 K to afford $[Cu(\mathbf{1})]^+$. Only the wavelength region 250-400 nm was analyzed affording log $K = 9.39 \pm 1.03$ (SPECFIT software).

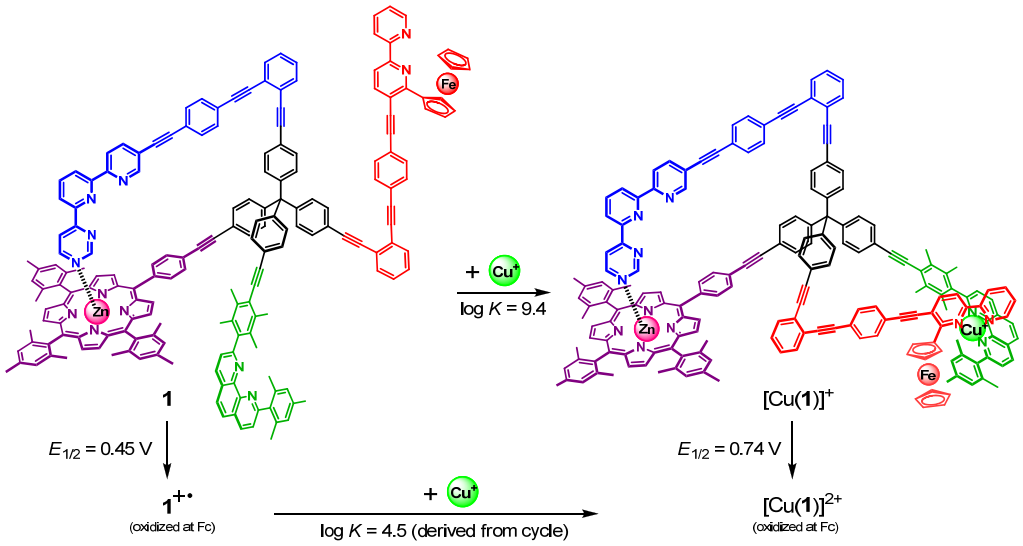

Figure S43. Hess cycle to predict the reduction of binding at the $[Cu(fcbipy^{+\bullet})(phenAr_2)]$ site in $[Cu(\mathbf{1})]^{2+}$. The change of binding strength by $\Delta\log K = 4.9 = 9.4 - 4.5$ implies detachment of the fcbipy arm from the $[Cu(phenAr_2)]^+$ unit.

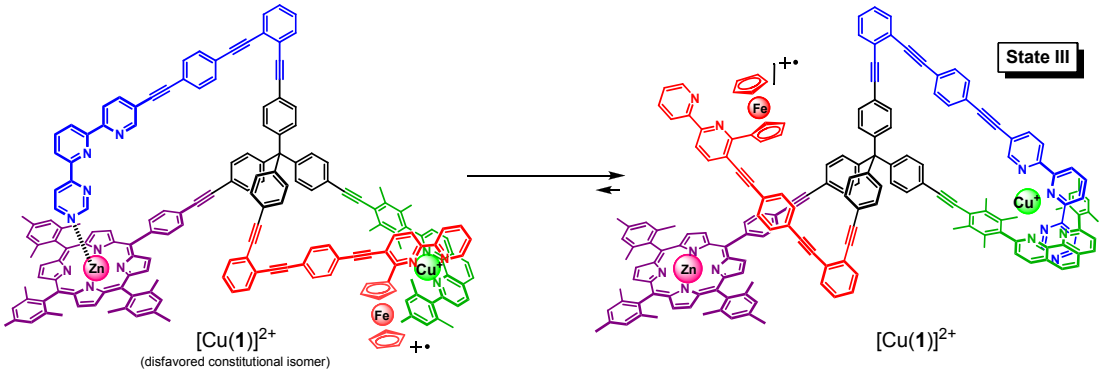

Figure S44. In $[Cu(\mathbf{1})]^{2+}$ (disfavored constitutional isomer) the $[Cu(fcbipy^{+\bullet})(phenAr_2)]$ complex is stabilized by log K = 4.5, whereas the $[Cu(azatpy)(phenAr_2)]$ complex in $[Cu(\mathbf{1})]^{2+}$ = State III has a binding strength of log K = 7.4 (approximated from that in $[Cu(\mathbf{7})]^{+}$).[3] From Δlog K = 2.9 one can derive that the equilibrium is 99.9% on the side of State III.

6. References

1 S. De, S. Pramanik and M. Schmittel, *Angew. Chem. Int. Ed.* 2014, **53**, 14255–14259.

2 (a) R. Breuer and M. Schmittel, *Organomet.*, 2012, **31**, 6642–6651; (b) R. Breuer and M. Schmittel, *Organomet.*, 2013, **32**, 5980–5987.

3 S. Gaikwad, A. Goswami, S. De and M. Schmittel, *Angew. Chem., Int. Ed.,* 2016, **55**, 10512–10517.